

The Space Experiment

G.G.S. / WIND / WAVES

Radio waves and plasma waves

1 - Description

L u c i e n S I T R U K

and

R o b e r t M A N N I N G

DOI <https://doi.org/10.25935/vps6-jb33>

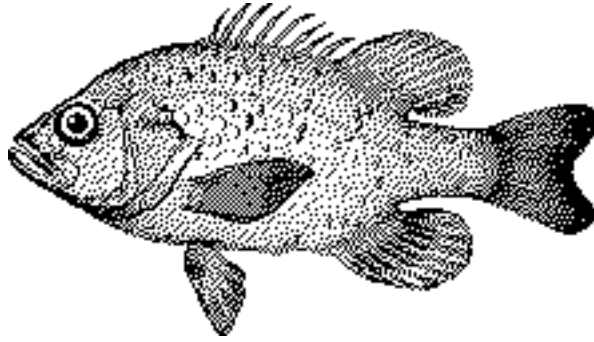
Publisher MASER/PADC

Citation Sitruk, L. & Manning, R. (2022) *The GGS/WIND/Waves Experiment* (Version 4.3, translated by A. Fave). MASER/PADC. [doi:10.25935/VPS6-JB33](https://doi.org/10.25935/VPS6-JB33)

License [CC-BY-4.0](https://creativecommons.org/licenses/by/4.0/)

*Space Research Department - DESPA
Plasma Physics Group*

Paris Observatory, Meudon.



is equipped with Faraday cups designed by MIT.

of the solar wind ion currents, from which the speed, density and temperature of the solar wind are deduced. AO: Announcement of Opportunity

Despa is supplying power transmitters and amplifiers to a magnetospheric sounder in Ibiza: with strong Swedish involvement. Despa will probably not be involved.

MIDEX

flyby Hecate ?

We are grateful to:

K. Goetz for his extensive explanations of the WIND/Waves software library and the DPU operating algorithm.

C. Meetre for summary plots and some documentation and software.

S. Chaintreuil and J. Hubert for their assistance with the computer system.

J. Tualy for his participation in the chapter on data access.

J.M. Boulben, D. Carrière, Y. de Conchy, R. Crépel, P. Fedou, S. Hoang, R. Knoll, A. Lecacheux, F. Leblanc, M. Maksimovic, N. Meyer, M. Moncuquet, G. Nicol, F. Pantellini, M. Poquerusse, J. Queinnec, M. Reiner, J-L. Steinberg, F. Wouters and P. Zarka for their contributions.

Contributions:

- Lucien Sitruk coordinated the drafting of this document, based on various written or oral sources, in an evolutionary manner.
- Several drafts were proofread, corrected and completed by Robert Manning, the instrumentation manager. Many of the instrumental and software descriptions are based on work done by R. Manning and his team.
- Jean-Louis Bougeret, P.I. of the WIND mission alternating with Mike Kaiser (GSFC), provided a lot of information on the Waves experiment for which he ensured the scientific support. He also reviewed the first test and provided many documents that explicitly served as reference material for this documentation.
- Claude Perche, who is in charge of the Waves data processing, contributed to the chapter on instrumental calibrations, and provided some plots.
- Liam Friel has provided a great deal of explanation of the TNR receiver and has written the processing algorithm.
- N. Monge provided clarification on the design of the RAD1/2 receivers and the calibration of the receivers.
- Philippe Richaume did a PhD thesis on the neural network of the TNR instrument, contributing to its validation and implementation.

This document has been produced at the Plasma Physics Group of the Space Research Department (DESPA), Unité de Recherche Associée 264 of the Centre National de la Recherche Scientifique (CNRS), at the Observatoire de Paris, section d'astrophysique de Meudon.

The French contribution to the GGS program is funded by the Centre National des Etudes Spatiales (CNES). This work has been carried out under CNES funding through the Institut National des Sciences de l'Univers (INSU).

Preamble

- This document describes the DESPA contribution to the WAVES experiment on board the WIND spacecraft. The Waves-2 part is not described. This text has been written progressively by compilation of various written or oral sources. As such, it may contain inaccuracies. In any case, please contact the people in France and in the United States who built the equipment or designed the instrument.
- This document is the first in a series of four documents:

I.	The GGS/WIND/Waves experiment:	1. Description.
II.	The GGS/WIND/Waves experiment:	2. Annexes.
III.	The GGS/WIND/Waves experiment:	3. Glossary of terms.
IV.	The GGS/WIND/Waves experiment:	4. Summary.
- See also reference [BOU94], which describes the WAVES experiment as a whole, special issues [SSR95], devoted to the description of the WIND spacecraft and the on-board instruments (or the corresponding hardcover book), and [GRL96], [ASR97], [GRL], for the first scientific results. Extensive information on the various ISTP missions, as well as a variety of online data, is available on the Web at <http://pwg.gsfc.nasa.gov>. The online documentation of the WAVES experiment includes the software library (also named “WindLib”) and the item documentation. In addition, the summary plots of the experiment and the daily dynamic spectra are available in the data processing room. Finally, the document [SIT93] presents the technical details of the calibrations performed in the United States.
- This version 4.3 follows versions 1.0, 2.0, 2.0.1, 3.0, 3.1, 3.2, 4.0, 4.1, 4.2 and 4.3. Paragraphs that are new, or have undergone significant changes from the previous version 4.3, are indicated by a thick vertical line in the text margin. The parts of the text in italics should be confirmed. The chapter on the physical quantities is undergoing major updates. The bibliography is in progress. This text was written using WORD5.1, on a Macintosh system. A Postscript version of this document is also available. This document is distributed at the DESPA level, plasma physics group. Any comments or suggestions to correct or complete this text are welcome.
- *This version has been translated by Agnès Fave and reviewed by Karine Issautier, Xavier Bonnin and Baptiste Cecconi.*

SUMMARY

The Waves experiment, aboard the WIND satellite, which was launched on November 1st, 1994 by NASA, is part of the American GGS (Global Geospace Science) program. This program is itself a component of the International Solar-Terrestrial Physics Program (ISTP).

During the first two years of the mission, the WIND spacecraft travels through the solar wind-Earth magnetosphere interaction regions, with an apogee of 80 to 250 R_e (Earth Radius, also noted in some figures as R_t , for terrestrial radius) and a perigee of 4.5 R_e . The scientific objectives of this mission are, among others, to locate the source of the solar wind, its physical and dynamical characteristics as it approaches the Earth, to study the energy dissipation mechanism, the non-linear behavior at the Earth shock, the radio mapping of the heliosphere, the analysis of the interaction of the fast and slow solar wind flows.

The satellite carries eight scientific instruments (six are American, one, Waves, is French, one is Russian) for wave, particle and gamma-ray analysis. The probe measures the characteristics of the solar wind: speed, density, composition, electric and magnetic field, temperature, charge and mass of ions and electrons.

The Waves experiment has two coplanar antennas in the ecliptic plane and one antenna along the rotation axis of the probe. An induction magnetometer designed by the University of Iowa and a fluxgate magnetometer, both mounted at the end of a long boom, allow the measurement of the dynamic and static magnetic field respectively.

The Waves experiment was developed jointly by Observatoire de Paris (Waves-1) and the University of Minnesota (Waves-2). The Waves-2 part includes the TDS (Time Domain Sampler) instruments for the analysis of extremely brief phenomena (up to 120 000 samples acquired per second) and FFT (Fast Fourier Transform), which provides the power spectra measured by the electric and magnetic antennas. The DPU controls all the equipment.

The Waves-1 part is described in this document. It includes the RAD1 [20 to 1040 kHz] and RAD2 [1.075 to 13.825 MHz] receivers for the detection of radio waves of solar and planetary origin. It also includes the Thermal Noise Receiver (TNR) covering the frequency range 4 to 256 kHz, divided into five frequency bands, for the analysis of quasi-thermal noise. To this end, this receiver is equipped with a sophisticated algorithm for signal analysis at high temporal and spectral resolution, as well as a formal neural network trained to track the local electron plasma frequency.

The telemetry of the Waves experiment is 936.96 bps at normal rate and double that at high rate. A software library (WindLib) allows access to the data. The Waves instrument has interconnections with two of the experiments on board WIND: 3D Plasma and SWE.

The first chapter of this document discusses the general characteristics of the WIND satellite and the Waves experiment. The second chapter describes the organization and data access of the Waves experiment. The third chapter presents, from an instrumental point of view, the RAD1 and RAD2 radio receivers and the measurement acquisition process. The fourth chapter describes the TNR receiver: this chapter is completed by several annexes. The fifth chapter presents the aspects of the physical quantities of the Waves receivers. A glossary and appendices are also provided.

Chapter I

GENERAL DESCRIPTION

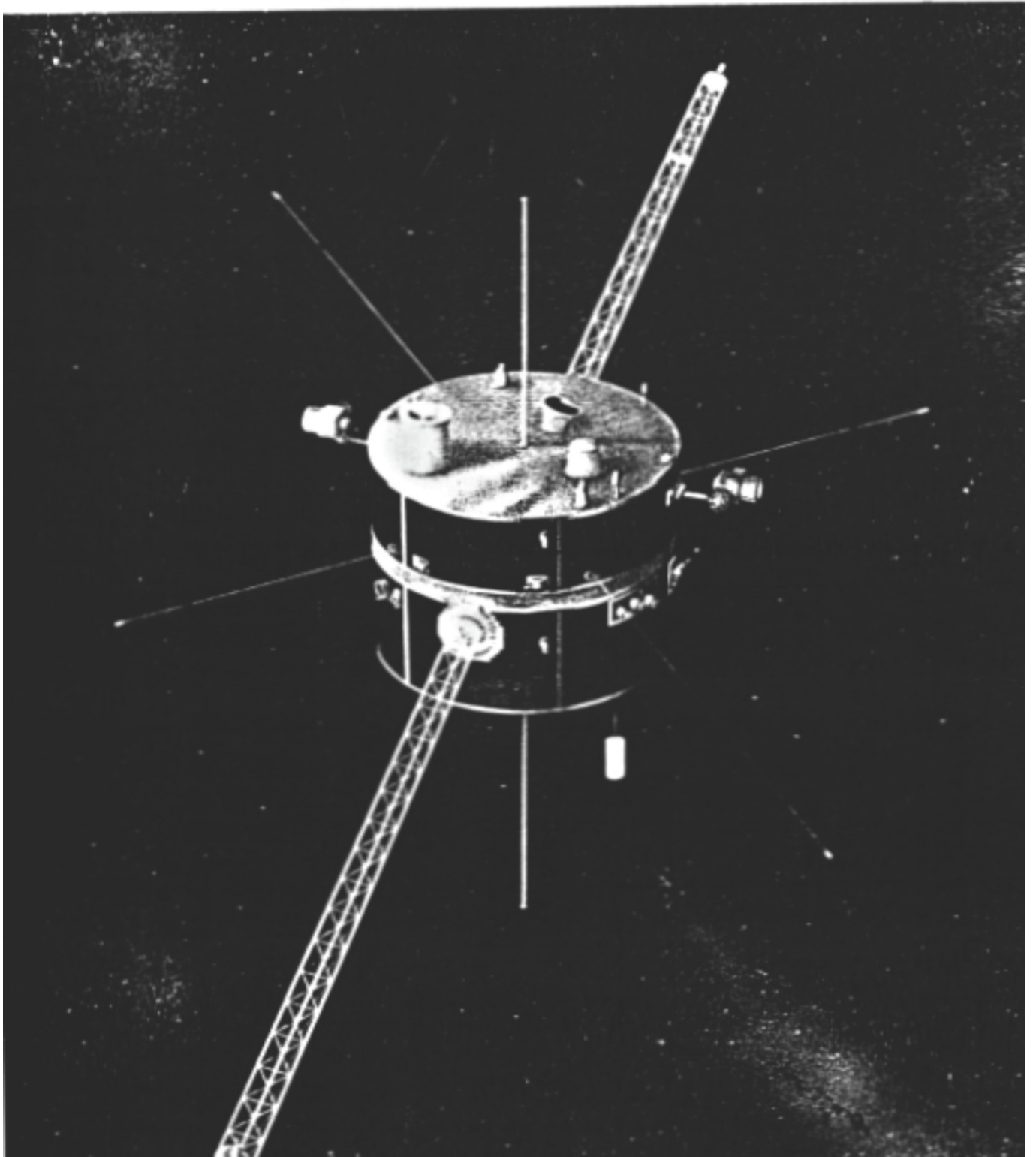
DOI	https://doi.org/10.25935/vps6-jb33
Publisher	MASER/PADC
Citation	Sitruk, L. & Manning, R. (2022) <i>The GGS/WIND/Waves Experiment</i> – Chapter 1 (Version 4.3, translated by A. Fave). MASER/PADC. doi:10.25935/VPS6-JB33
License	CC-BY-4.0

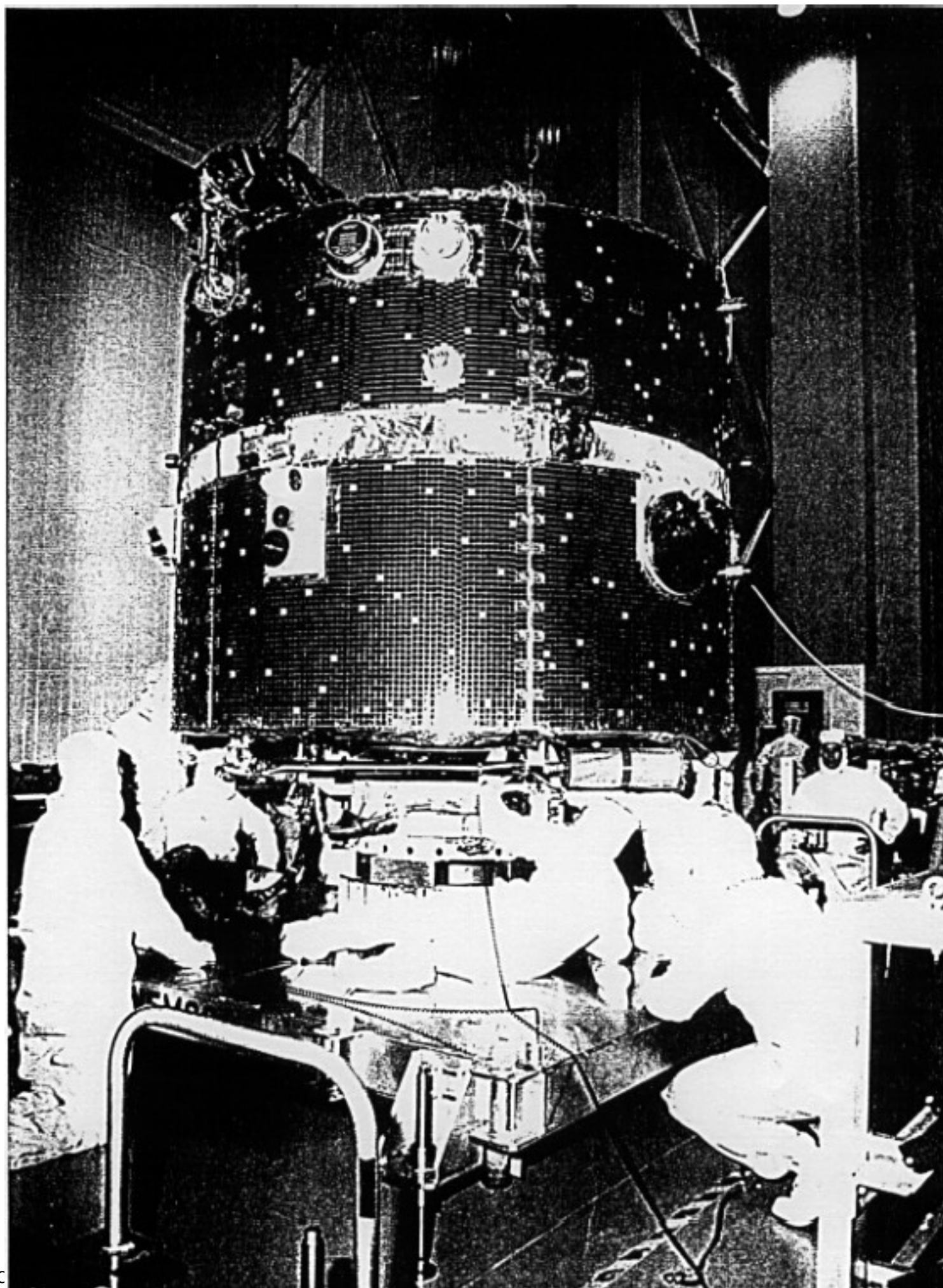
Summary

The WIND interplanetary probe, launched on November 1st, 1994, aims to analyse the solar wind and its relationship with the Earth's magnetosphere. This mission forms, with the POLAR mission, the GGS program, the American contribution to the International Solar-Terrestrial Programme ISTP. The WIND mission is also associated with solar-related Earth disturbance prediction programs. Throughout the mission, the probe flies over different regions of the solar wind, where it is most often found, and the magnetosphere, lying in the plane of the ecliptic. As part of the multi-platform measurements of the ISTP program, the WIND probe provides information on the state of the solar wind at a given time. The satellite, stabilized by rotation (3 seconds per rotation), carries eight scientific instruments for the analysis of waves, solar wind particles and gamma rays. DESPA is contributing to this mission as part of the Waves experiment, in collaboration with GSFC and the University of Minnesota. This experiment includes the RAD1 [20 kHz, 1040 kHz] and RAD2 [1075 kHz, 13825 kHz] radio receivers, the TNR [4 kHz, ca. 256 kHz] thermal noise receiver, the TDS waveform receiver, which is capable of sampling the signal at very high rates, and the Fast Fourier Transform, FFT, receiver. The whole experiment is controlled by a central microprocessor, the DPU. The Waves experiment is connected to two equatorial antennas (2 x 7.5 m and 2 x 50 m), an axial antenna (currently 2 x 4.65 m) and a triaxial induction magnetometer.

Content

1. GENERAL DESCRIPTION	10
1.1. General framework of the WIND mission	10
1.1.1. The GGS program	10
1.1.2. Other related missions and programs	12
1.1.3. Multi-point measurements - Analysis at different scales	13
1.2. Features of the WIND mission	15
1.2.1. Launching the probe	15
1.2.2. Orbital characteristics	17
1.2.3. Technical data of the probe	21
1.2.4. Detection and prevention of solar disturbances	23
1.2.5. Experiments on board the WIND probe	25
1.3. The Waves Experiment	28
1.3.1. Project milestones.....	28
1.3.2. First maneuvers.....	28
1.3.3. scientific objectives and applications	29
1.3.4. Main participants and distribution	32
1.4. General description of the instrument	32
1.4.1. Electric antennas	33
1.4.2. Magnetic field measurements.....	39
1.4.3. Solar Impulse	41
1.4.4 The Waves Experiment	42





1. GENERAL DESCRIPTION

1.1. General framework of the WIND mission

1.1.1. The GGS program

The Waves¹ experiment, aboard the WIND satellite², launched on 1 November 1994, is part of NASA's multi-satellite GGS program: *Global Geospace Science*. This program is itself a component of the International Solar-Terrestrial Physics Program (ISTP) of NASA, ESA and ISAS, which covers the following topics: sun and solar dynamics, solar corona, origin of the solar wind, sun-earth relations, plasma flow, earth environment and geospace interactions.

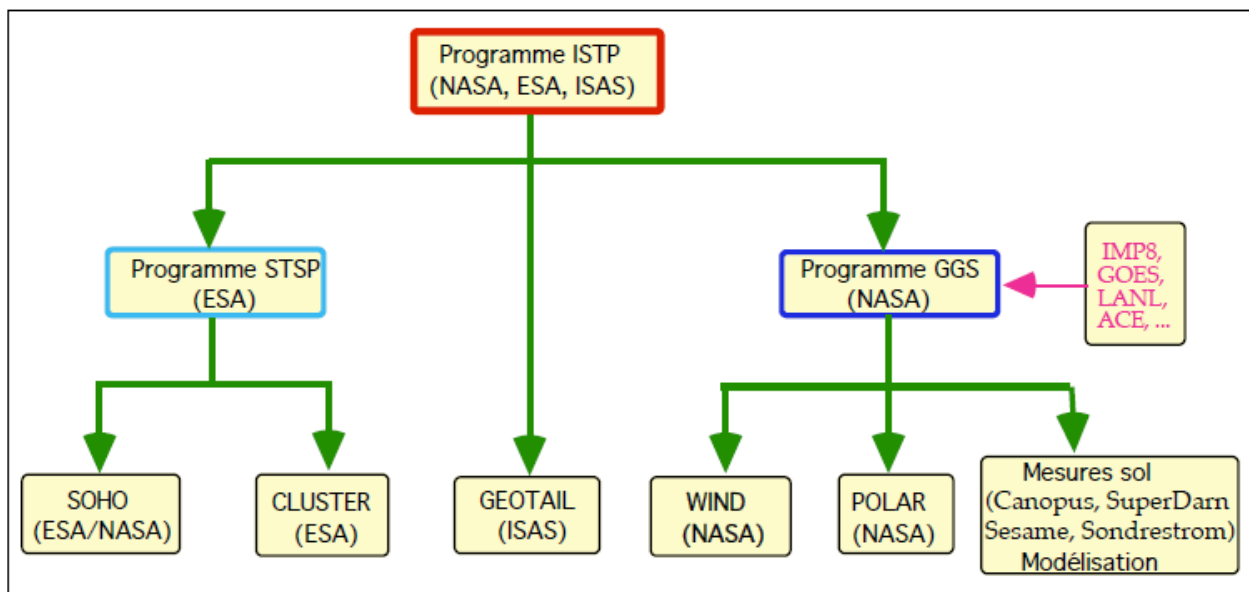


Fig. 1-1 : Missions of the ISTP

The GGS program is managed by the GSFC (Goddard Space Flight Center, Greenbelt, Maryland) at NASA Headquarters in Washington³. It is an update of the former US program OPEN: Origins of Plasmas in the Earth's Neighborhood. This program initially consisted of four satellites⁴ which were to fly over different regions: the solar wind and the upstream IP environment, the polar regions, the equatorial magnetosphere and the distant magnetotail. In 1983, Europe with SOHO and CLUSTER, and Japan joined the project. The OPEN program was renamed GGS and the four satellites renamed respectively WIND, POLAR, EQUATOR (to be provided by NASA) and GEOTAIL (to be provided by ISAS). The whole project was merged to become the ISTP program. In 1986, the EQUATOR

¹ References can be found in [BOU88], [BOU92], [BOU95], [CEL88], [KAI], [GGS90], [MEE].

² A satellite is a device (artificial satellite) or a celestial body (natural satellite) in orbit around a massive body. A space probe is an artificial construction designed to investigate celestial objects. WIND is therefore more a space probe than a satellite. We will not distinguish the two terms in this document, as this abuse of language seems to have become commonplace.

³ The total cost of the WIND mission is \$173 million, or about 1 billion francs. The cost of the ISTP program to NASA has been estimated at \$640 million.

⁴ IPL (Interplanetary Physics Laboratory), PPL (Polar Plasma Laboratory), EML (Equatorial Magnetosphere Laboratory) and GTL (Geomagnetic Tail Laboratory).

mission was cancelled for budgetary reasons. In compensation, a small satellite named EQUATOR-S (S for Small), designed to perform in situ equatorial measurements, and to cover some of the objectives originally assigned to the EQUATOR satellite, is scheduled for early 1998. The French participation in the GGS program includes the WAVES (DESPA, Meudon) and 3-D Plasma (contribution of CESR, Toulouse) experiments in the framework of the WIND mission, and TIDE (contribution of CETP, Vélizy) in the framework of the POLAR mission.

The objective of the GGS program is to quantify the behavior of coupled solar wind/earth magnetosphere/earth ionosphere systems. It concerns more particularly the study of the transfer of energy, mass and momentum from the interplanetary medium into the geospace, the interaction between the different components of the medium, the impact of the solar wind on the terrestrial environment. This program consists of the two missions WIND and POLAR. The objective is to carry out high resolution measurements, each satellite flying over different regions of interest. The WIND satellite is designed to study the solar wind and its relationship with geospace. It seeks to determine the sources, acceleration mechanisms and propagation processes of energetic solar wind particles. It provides data on solar wind parameters (waves, particles, magnetic field) for magnetospheric and ionospheric studies. It determines the magnetospheric response to interplanetary upstream space. It provides the basic observations in the ecliptic plane necessary for the study of heliospheric physics, in the framework of comparative studies with the ULYSSES probe. The POLAR satellite is designed to study the interaction of the solar wind with the Earth's upper atmosphere (polar auroras)⁵. It was launched into polar orbit on 24 February 1996, thus making the entire GGS program operational. The GGS program also takes into account equatorial data from the GOES⁶ (Geostationary Operational Environmental Satellite) series of geostationary meteorological satellites of the National Oceanic and Atmospheric Administration (NOAA, Department of Commerce) and the LANL (Los Alamos National Laboratory, Department of Energy) series of satellites.

Ground and space-based observations are complementary (see also § 1-3-4: ground-space synergy). This is why the GGS program also includes ground-based observation facilities, equipped with coherent and incoherent radars, photometers, magnetometers, optical and imaging instruments, especially for aurora, etc. These means are:

- The DARN/SuperDARN (Dual Auroral Radar Network), an international network of coherent radar sites located in the high latitudes of the Earth (Northern Hemisphere, Antarctica).
- The Canadian Auroral Network for Open Program Unified Study (CANOPUS) in central Canada⁷. This network was designed in the 1980s as ground support for the OPEN program. Measurements from this coherent radar network are to be integrated into the WIND/Waves software library in the near future.
- SESAME (Satellite Experiments Simultaneous with Antarctic MEasurements) based at Halley Station, Antarctica.
- The Sondrestrom Radar Facility at Sondre Stromfjord, Greenland.

Finally, a new program, GGS/SOLARMAX, has been proposed [IST97], with the objective of being part of the NASA Sun-Earth Connection (SEC) program [SUN97], along with ten other satellites already in operation or planned. The purpose of this program is to study the sun-earth relationship during periods of intense solar activity (next solar maximum expected from 1999 to 2001). The SEC program is itself a component of the American inter-agency NPWP (National Space Weather Program)⁸, in which NASA is playing a pioneering role in space exploration, and whose objective, in

⁵ The FREJA, INTERBALL auroral probe, POLAR and FAST missions are currently dedicated to the physics of small and medium scale phenomena in auroral and adjacent regions at different altitudes.

⁶ The GOES satellites analyze X-rays and solar particles.

⁷ Canadian Space Agency (CSA). Network of remote sensing devices located at 13 different sites west of Hudson Bay. It includes magnetometers, riometers, scanning photometers, digital panoramic imager, and auroral radar.

⁸ The following US government agencies: Department Of Commerce (DOC) and NOAA,, Department Of Defense DOD, Department Of Energy (DOE), Department Of Industry (DOI), NASA, and the National Science Foundation (NSF), are stakeholders

the next decade, is to gather observations that will make it possible to establish reliable quantitative forecasts of earth-sun interactions (see also § 1-2-4-2). The GGS/SOLARMAX program would build on the existing resources of the GGS⁹ program.

1.1.2. Other related missions and programs

In addition to the GGS program, NASA is collaborating with ISAS and ESA in the COSTR (Collaborative Solar-Terrestrial Research) program on the GEOTAIL (ISAS), SOHO (ESA/NASA) and CLUSTER¹⁰ (ESA) missions. The latter two missions constitute the Solar Terrestrial Science Program (STSP) for ESA, the first of the four "cornerstones" of ESA's Horizon 2000 program. The GGS and COSTR programs form the two important components of the ISTP program. They also incorporate ground-based observations, as well as theory and modelling tools¹¹. The GEOTAIL (GEOMagnetic TAIL) satellite was built in Japan and launched by NASA on 24 July 1992. Its purpose is to study the plasma in the Earth's magnetospheric tail. The CLUSTER mission, which consists of a flotilla of four identical satellites arranged in a tetrahedral geometry, is designed to study the microphysics of plasma turbulence in the boundary regions of the Earth's magnetosphere, as well as to explore the little-known regions of the polar horns. Finally, the SOHO (Solar and Heliospheric Observatory) probe, a heliocentric satellite of ESA, is designed to study the internal structure of the sun, the solar corona, and the origin of the solar wind. Launched on December 2, 1995, it is permanently positioned at the L1 Lagrange point.

Other missions are also attached to the ISTP program, in particular INTERBALL (launch on August 3, 1995 for Interball Tail probe, and on August 29, 1996 for Interball Auroral probe), by the former Russian InterCosmos organization (IKI). The S/C IMP8, launched in 1973, is still in operation. It allows the measurement of the magnetic field, plasma parameters, properties of energetic particles and cosmic rays. Located close to the Earth's magnetosphere, it is a reliable indicator of the state of the solar wind when it meets the Earth's magnetosphere. About 60% of the data it acquires comes from the solar wind, 40% from the magnetosphere and magnetotail. Other satellites, such as ACE (Advanced Composition Explorer), or FAST (Fast Auroral Snapshot Explorer) are to join the GGS program. FAST was launched on August 21, 1996, in a polar orbit (400 x 400 km), with the objective of studying the plasma physics of the Earth's auroral regions in detail. The S/C ACE was launched on August 25, 1997, with the objective of analyzing the composition of the solar wind at L1. Another example is the ULYSSES probe, for which DESPA designed and built the URAP radio receiver. This probe was launched on October 6, 1990, with the objective of making measurements of the solar wind at high heliocentric latitudes¹² [ESA]. The S/C observations of the ISTP program are complemented by images in the hard and soft X-ray range of the Sun and a spectroscopic analysis of the coronal activity of the Japanese S/C YOHO. The missions mentioned so far concern the study of the Sun, the Sun-Earth relationship and the Earth's magnetosphere. Let us add that within the framework of the studies of the comparative magnetospheres, DESPA also cooperates in programs such as CASSINI/HUYGENS (Saturn magnetosphere), or MERCURY ORBITER (Mercury magnetosphere). These international contributions are coordinated by the IACG: Inter-Agency Coordination Group for

in this program.

⁹ As such, it should not represent any additional cost (development cost, delays, launch cost, etc.) for NASA.

¹⁰ Initially scheduled as part of the first qualification launch of the Ariane rocket (Ariane 501), this mission could not achieve its objectives because of the failure of the launcher. The launch of the probes was rescheduled for the year 2000, using Russian Soyuz rockets. In the framework of this mission, DESPA collaborates with CETP and LPCE on the STAFF (Spatio-temporal Analysis of Fluctuating Fields) experiment.

¹¹ These tools are used to model the Earth's magnetosphere: a large-scale fluid approach using magnetohydrodynamic (MHD) theory, non-collisional particle kinetic theory using the Vlasov equation, or hybrid models combining these two approaches for a medium-scale description. Four teams are involved in the modeling and theory aspects of the GGS program: the University of California at Los Angeles (UCLA), the University of Maryland (USA), Dartmouth College, and the University of Alaska.

¹² This probe took advantage of the gravitational potential of the planet Jupiter to extract itself from the ecliptic plane (the "gravitational slingshot" effect).

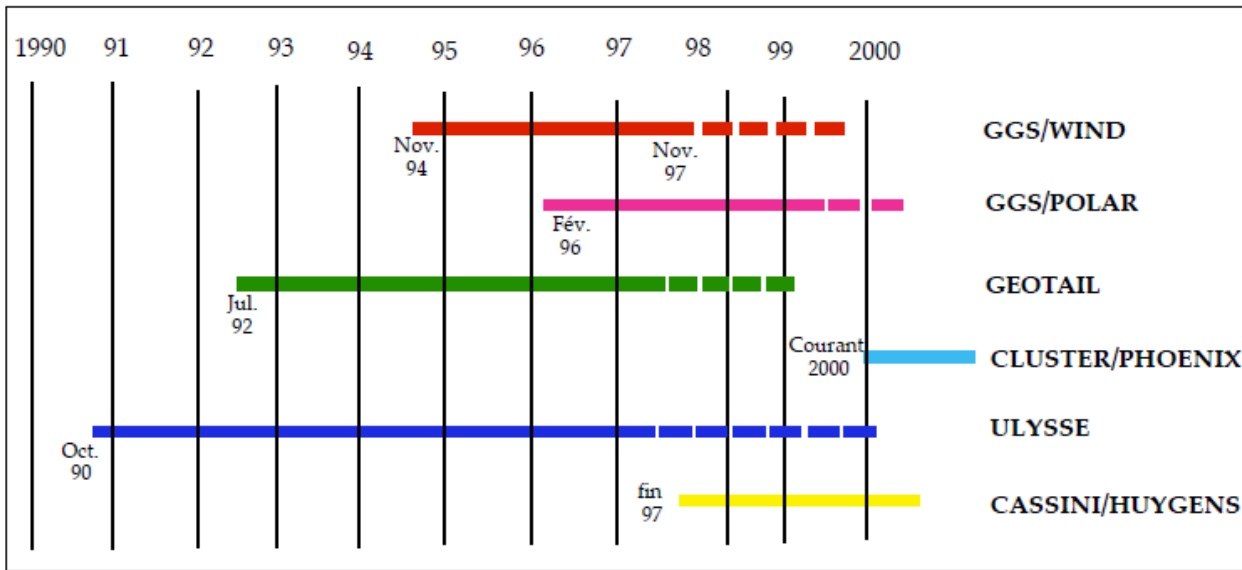


Fig. 1-2: Dates of different missions

The table above presents timelines of these main missions. Among them, DESPA participates in the ULYSSES (ESA/NASA), WIND (NASA), CLUSTER/PHOENIX (ESA/NASA) and CASSINI/HUYGENS missions (NASA/ESA). The dates after 1997 are the principle dates retained by the agencies: We briefly describe these various missions in the glossary.

1.1.3. Multi-point measurements - Analysis at different scales

The comparison of measurements acquired by satellites distributed over key regions of the interplanetary medium is a key objective of the ISTP program. The satellites of the ISTP missions are typically 10 to 100 R_e apart. This spatial dissemination makes it possible to highlight correlations between measurements, and thus to better understand the chain of solar wind-Earth magnetosphere coupling phenomena on a large scale [HOF96]. In particular, the possibility of following the progression of disturbances in the interplanetary medium is particularly useful, cf. § 1-2-4.

Analysis of a sequence of data from a single satellite does not tell us whether an observed phenomenon is due to time-dependent variations (such as the detection of an isolated disturbance) or to changes in the structure of the environment over which the probe is flying (such as the crossing of boundary regions of the magnetosphere). To overcome this space-time ambiguity, missions such as ISEE, and recently INTERBALL, have deployed satellites in pairs¹⁴.

The small and medium scale study of the Earth's magnetosphere is envisaged within the framework of the CLUSTER mission, one of whose objectives is to carry out the first three-dimensional analysis by comparing the measurements of four identical, non-coplanar satellites, separated from each other by a few hundred to several thousand km, i.e., 1 R_e or less, making simultaneous measurements. The

¹³ Founded by the four major space agencies NASA, ESA, ISAS and IKI, the group's first objective was to coordinate space missions to Halley's comet in 1986. The new objective of the IACG is the coordination of research on the physics of the Sun-Earth relationship. This group brings together the heads of the four main space agencies (ESA, IKI, ISAS, NASA). The ISTP program is also called IASTP, to emphasize the role of this agency in approving, launching, and coordinating these various missions. The IACG defines research campaigns on particular themes. For example, ...

¹⁴ Initially, the OOE (Out Of Ecliptic) mission, which was the origin of the Ulysses mission, was to comprise two twin satellites. After the gravitational assistance of the planet Jupiter, one was to head towards the solar south pole, the other towards the north pole, and then each satellite was to ascend towards the pole opposite to the one initially flown. This trajectory allowed a stereoscopic analysis of the heliosphere by simultaneous measurements in each hemisphere [ROT97].

conformation of the swarm and the distances between the probes will be regularly adapted to the characteristics of the overflow regions of the magnetosphere. The simultaneous presence of four satellites equipped with the same instruments should allow the spatio-temporal decoupling, on a small and medium scale, of the physical phenomena observed.

It should be noted that the analysis of large and small scale structures are two complementary aspects of the study of geophysical plasmas.

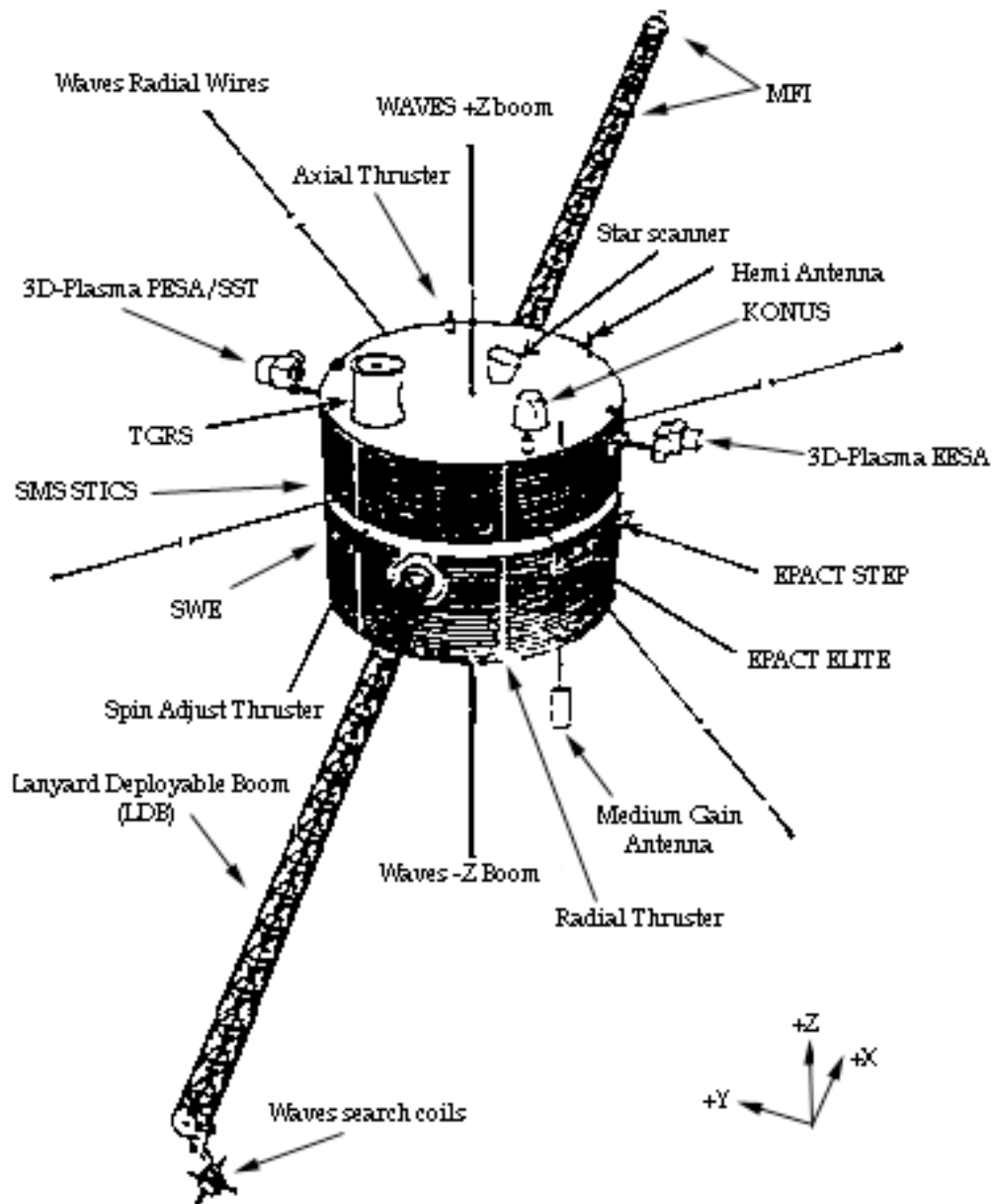


Diagram of the WIND satellite (from Space Science review, vol 7, no 1/4 Feb. 95)

The following elements are shown on this diagram (for obvious reasons of perspective, not all elements have been shown):

- Components required for the satellite itself (see § 1-2-3)

The Medium Gain Antenna (MGA) for communication of telemetry data to the ground, as well as a hemispheric beam antenna for early orbit operations and contingencies.

The star tracker to determine the attitude of the probe.

Thrusters: axial, radial, rotation adjustment, which are used for satellite maneuvering.

- Electromagnetic sensors (see § 1-4-1 and 1-4-2)

The LDB (Lanyard Deployable Boom), a 2 x 12 m boom supporting the two magnetic field sensors: the fluxgate magnetometer (MFI experiment) for a quasi-static field measurement, and the search coils magnetometer (Waves experiment).

The electrical antennas of the Waves experiment: axial antennas in +/- Z directions, and two equatorial wire antennas.

- Sensors for ion, electron and gamma ray experiments (see § 1-2-5)

The PESA/SST, EESA electrostatic particle analyzers of the 3DP particle experiment.

Instruments for the analysis of gamma-ray bursts: TGRS, KONUS.

EPACT STEP (SupraThermal Energetic Particle telescope) and ELITE (ELectron Isotope TElescope).

The SWE experiment (only the part located on the lower structure of the satellite).

The STICS instrument of the SMS experiment.

1.2. Features of the WIND mission

1.2.1. Launching the probe

The WIND spacecraft was launched¹⁵ on Tuesday, November 1st, 1994 at 10:31 a.m. Paris time (23:31:00 UTC) from the U.S. Cape Canaveral Air Force Center (CCAFC) on Florida's east coast.

The probe was launched using a Delta II ELV¹⁶ rocket. The photograph below shows the launch of the WIND probe on this rocket. The rocket is a three-stage launcher, 38.2 m high and 2.4 m in diameter, with the first two stages using liquid fuel and the third stage using solid fuel (payload support module). The first stage has nine auxiliary solid rocket boosters on its sides. There is an interstage, a second stage, and the upper or third stage and the payload protection fairing, which is three meters in diameter.

The first stage of the rocket operates for 256 seconds. The second stage flies over Africa to a "parking" orbit, the third stage places the payload in a highly elliptical orbit. The time between launch and satellite separation is about 1 hour and 21 minutes. The launch azimuth is 95°.

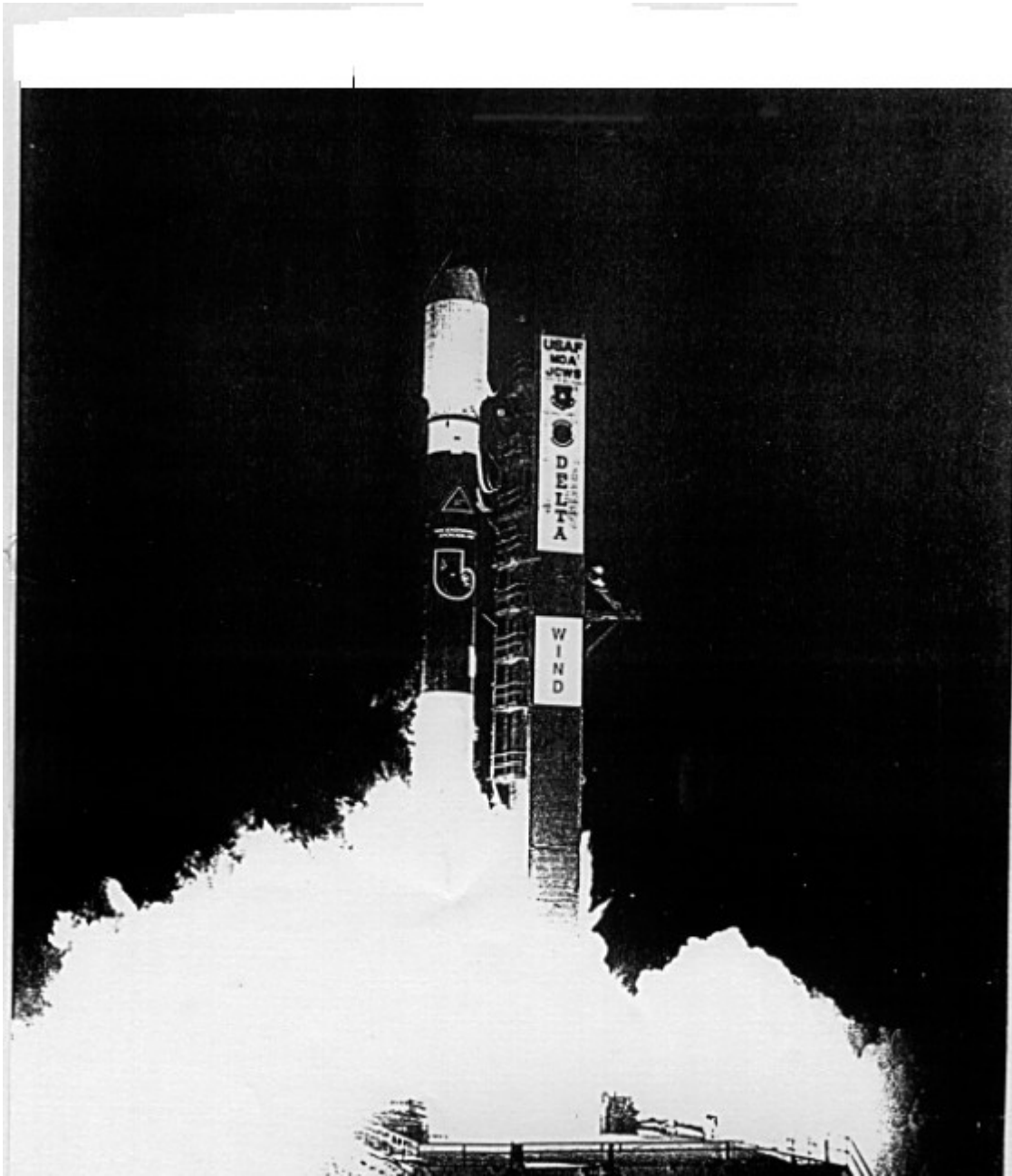
The duration of the WIND mission is a minimum of three years ("nominal" duration), at full capacity. The mission should therefore continue until November 1997. A follow-up to this mission is under study, with different trajectory scenarios, see above.

The launch of the WIND probe occurred during the current solar minimum.

Launch of the WIND probe aboard the DELTA II rocket

¹⁵ The launch took place two years later than originally planned (initial launch in December 1992), due to technical problems. The launch window was five minutes (these launch windows are related to the handling aspects of the launcher and/or ballistic conditions).

¹⁶ ELV: Expendable Launch Vehicle: a space vehicle used only once. There are two versions of the Delta II rocket, the 6925 and 7925, the more powerful version. The 7925-10 version is the one used for this launch. The rocket was built by McDonnell Douglas Astronautics Company (Huntington Beach, CA) under the technical direction of GSFC/NASA. For comparison, the other main families of launchers today are: the American Atlas and Titan rockets, the Chinese "Long March" rockets, the European Ariane IV and V rockets, the Russian Proton and Soyuz rockets.



1.2.2. Orbital characteristics

The orbital characteristics of the WIND probe have been chosen to allow radial mapping of the interplanetary environment around the Earth. In the first weeks after launch, the probe describes highly elliptical orbits around the Earth ("phasing loops"), very eccentric to the Earth (high orbital eccentricity): perigee¹⁷ is 6750 km, apogee 43000 km, inclination 28.7°. The satellite makes 4.5 such orbits¹⁸. During the mission, the probe describes the solar wind-magnetosphere interaction regions with an apogee of 80 to 250 R_e, and a perigee of at least 4.5 R_e (i.e. 29 000 km).

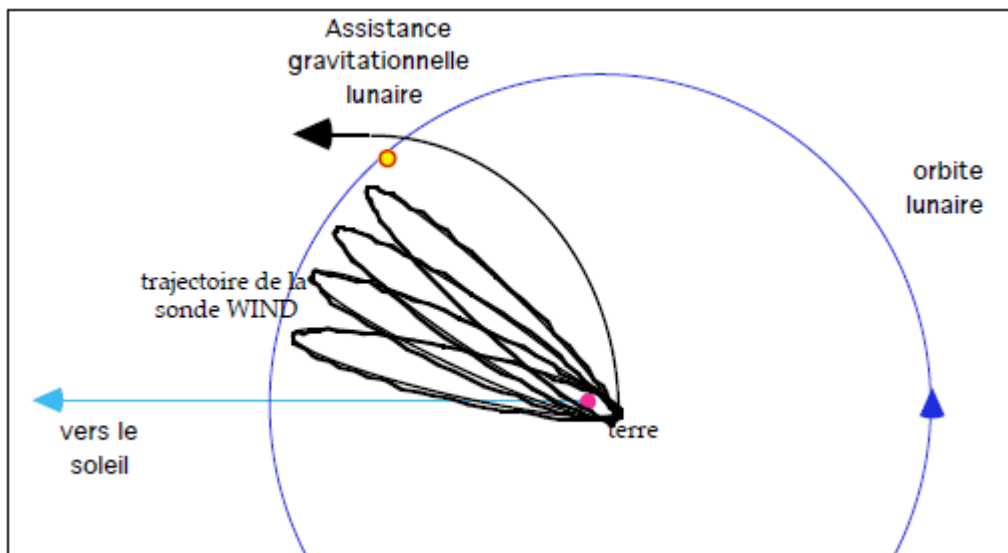


Fig. 1-6: Double lunar gravitational assistance (trajectory projected in the ecliptic plane).

Double, periodic, close encounters with the moon take advantage of its gravitational attraction to keep the apogee close to the earth-sun line during the mission: double lunar swing-by (DLS)¹⁹.

This orbit keeps the satellite above the Earth most of the time. This means that the WIND satellite spends much of its time away from Earth disturbances (such as ions reflected from the Earth's shock).

This technique makes it possible to fly over the various magnetospheric regions as well as the solar wind with a minimal quantity of fuel [FAR81]. In principle, the WIND probe was to reach the L1 Lagrange point in February 1997, and to remain there for at least one year, until the end of the mission. Located permanently in the solar wind, it was to perform a continuous analysis of the solar wind, about one hour before it hit the Earth's magnetosphere. This probe can thus play the role of a "sentinel" to warn of the effects of the solar wind on the Earth's environment ("monitoring").

Just as other missions have been extended in the past²⁰, an extension to the WIND mission is

¹⁷ The perigee is the top of the trajectory closest to the Earth, the apogee is the farthest top.

¹⁸ There are thus four perigees, i.e. four passages close to the Earth, as well as four apogees, before the first lunar gravitational assistance. At each perigee, the probe grazes the plasmasphere, which allowed in particular the study of Bernstein modes in the plasmasphere [MON]. The close passage near the moon on December 27, 1994, at about 6.8 lunar radii (1 RL \approx 1738 km), in the "antisolar" direction, also allowed the study of the interaction between the solar wind and a massive body ("lunar wake") [GRL].

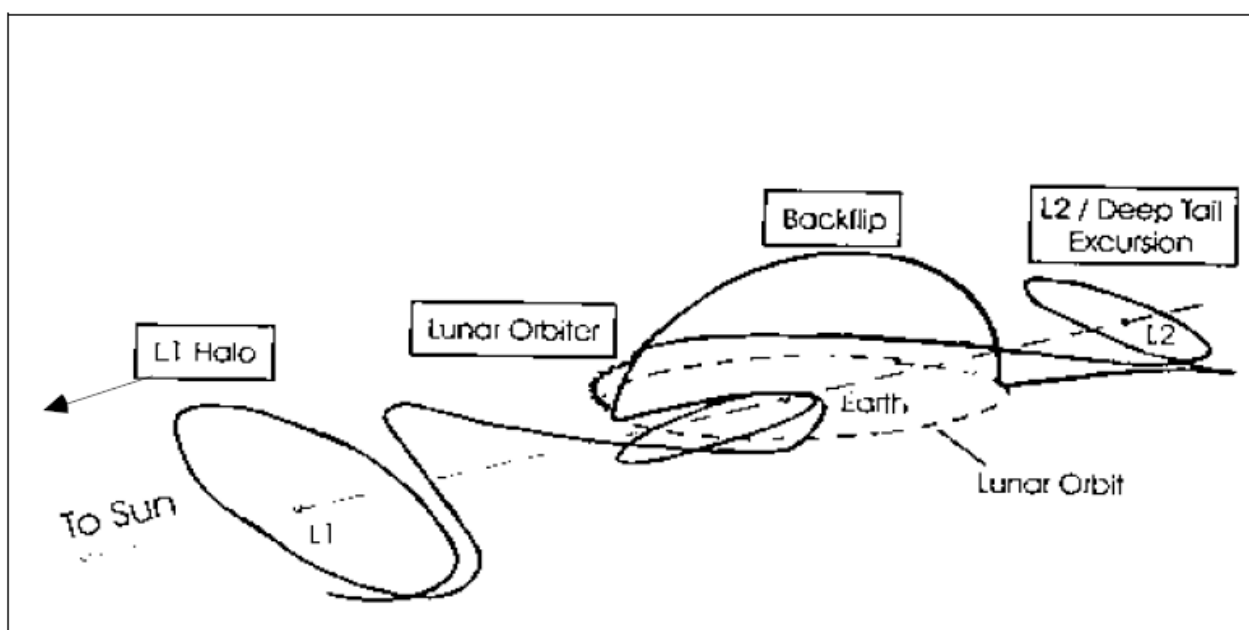
¹⁹ This technique has also been used by the Geotail satellite to continuously maintain its apogee in the magnetotail. This technique is inexpensive in terms of propellant, but it assumes that it is possible to approach the moon under appropriate geometric and kinematic conditions; the lunar gravitational attraction then makes it possible to bend the probe's trajectory according to the needs of the mission.

²⁰ The new Ulysses mission, UMSM (Ulysses Mission to Solar Maximum), coincides with a period of maximum solar activity. Similarly, the ISEE3 probe, after having stayed at the Lagrange point, became the ICE (Interplanetary Comet Explorer) probe,

envisaged. This would consist of four phases: starting from the halo orbit at Lagrange L1 (phase 1), the spacecraft would reach Lagrange L2 by means of a back-flip maneuver (phase 2), with exploration of the magnetotail: deep tail excursion phase (phase 3). The backflip technique, already used to transfer the ISEE3 probe from L1 to the magnetotail, allows the transition from a daytime DLS orbit to a nighttime DLS orbit. It is fast, efficient, and avoids a conventional, more energy-intensive orbit transfer²¹. It would allow, among other things, the study of emissions from Earth (AKR, LF bursts). An additional extension, more costly in energy, consisted in placing the probe in orbit around the Moon: "lunar orbiter" (phase 4), using this star as an occultation disk, which would have had the advantage of sheltering it from solar radiation and would have made it possible to study various galactic and extra-galactic radio sources, fast pulsars etc...

It is now thought that the WIND probe will be maintained in its current type of orbit, which appears to be of greater scientific interest. It is therefore not expected that the probe will eventually stay at the L1 Lagrangian point, as originally planned. As WIND remains in the solar wind most of the time, the ISTP satellite community can use the information from WIND for benchmarking purposes as reference data on the state of the solar wind.

Another scenario is proposed under the GGS/SOLARMAX program.



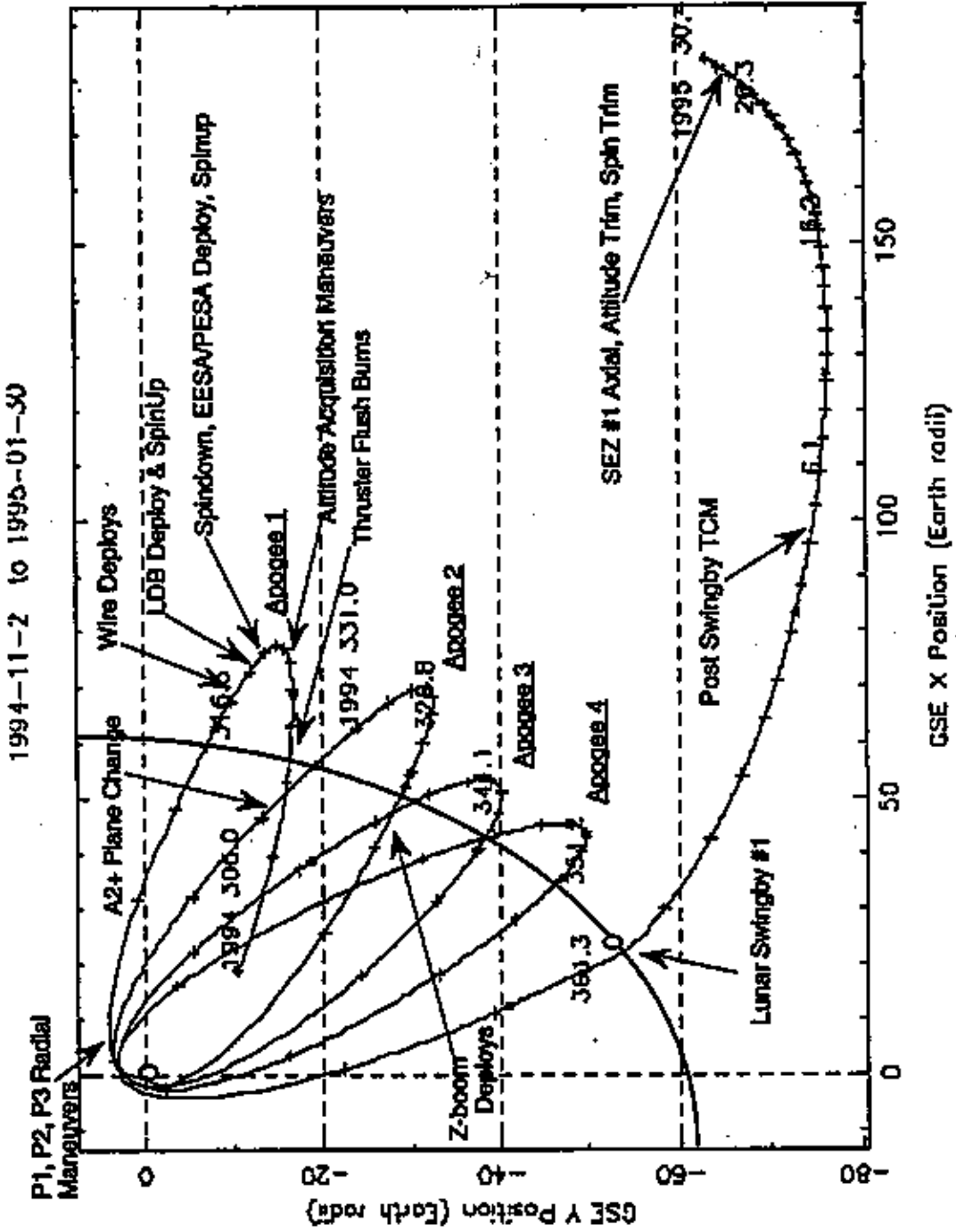
WIND probe trajectory: mission extension project.

during its new mission to the Gacobini-Zinner comet.

²¹ In a two-body orbit transfer, the reorientation of the apogee from the night side to the day side corresponds to a 180° change in the perigee argument, which is very energy intensive.

WIND Trajectory (1 of 2)

LOCKHEED MARTIN



WIND probe trajectory: general trajectory

1.2.3. Technical data of the probe

WIND, like the POLAR probe, is a traditional satellite design, with a basic cylindrical structure, 2.4 m in diameter and 1.8 m high²². It is stabilized by rotation around its main axis: gyroscopic stabilization²³. The axis of rotation is kept normal to the plane of the ecliptic to within one degree for the duration of the mission, thus optimizing the performance of the on-board instruments and the communication system.

Speed of rotation	20 rotations per minute ²⁴ : 1 rotation in 3 s
Weight	1158 Kg of which 278,9 Kg of fuel
Diameter	2,44 meters approximately
Height	1.88 meters approximately

On board a satellite, there are a number of components called "subsystems". On board the WIND satellite, the following "subsystems" can be found, in a rather classical way:

- **Power supply subsystem:** the satellite consumes energy which must be generated, stored and distributed. It is supplied with energy by solar cells²⁵ (photovoltaic cells) lining the solar panels that cover the satellite. This energy is abundant outside eclipse periods (satellite in the shadow of the Earth or Moon). The total surface area of the solar cells is 11.5m², giving the satellite a maximum power of 472 Watts, including 144 Watts for the payload. In order to guarantee a constant level of electrical power, the on-board accumulators (batteries) store the necessary energy during periods of sunlight, which they release during periods of shadow or eclipse. In this case, the satellite orbit is designed so that the eclipse duration does not exceed 90 minutes, a constraint that also takes into account aspects related to the thermal control of the satellite (see below).
- **Structure and Thermal Control Subsystems:** The structure of the satellite refers to the mechanical assemblies of the satellite that perform static or dynamic functions. The basic shape of the satellite is cylindrical. The curved outer panels divide the circumference into 6 segments. The solar panel array is an integral part of the structure and provides a significant portion of the required rigidity. Thermal control consists in maintaining the satellite equipment within a fixed temperature range, in order to avoid their degradation, which would limit the life of the satellite. This control is achieved passively by means of coatings and multi-layer insulation.

Attitude Control And Determination Subsystem (ACADS)²⁶ : external forces (Earth's magnetic field, electric fields, disturbances external or internal to the satellite, aerodynamic drag, solar radiation, etc.) can cause attitude perturbations. The ACADS subsystem is designed to perform

²² The WIND satellite was built by Martin Marietta Astro Space, Princeton, New Jersey ("prime contractor"), now Lockheed Martin (Sunnyvale, California)-TBC.

²³ This is also referred to as a spin-stabilized satellite or "spinning" satellite. In the absence of acting external torques, the direction of the satellite's axis of rotation remains fixed because the angular momentum must be conserved. The attitude will therefore be preserved. This is a form of satellite stabilization known as passive stabilization [CEL95]. Another technique consists of a three-axis stabilization. Gyroscopic stabilization allows continuous scanning for field and particle measurement instruments.

²⁴ The WIND probe performs 20 rotations per minute to allow sampling of the ambient charged particle distribution function with good time resolution. In fact, there are 19.38 rotations per minute i.e.: $60/19.38 = 1$ rotation in 3.096 s.

²⁵ Photovoltaic cells convert solar energy into electrical energy.

²⁶ Attitude is the orientation of a system of axes related to the satellite with respect to external reference points: the earth, the sun, or more generally with respect to astronomical reference points assumed to be fixed.

all orbit and attitude corrections necessary to maintain the satellite's position within specified limits throughout the mission. This subsystem consists of two horizon sensors (used during early orbit operations), two sun sensors, an accelerometer, a star tracker²⁷ for accurate attitude information.

- **Communication Subsystem:** telemetry, satellite remote control²⁸. WIND's main communication antenna is a Medium Gain Antenna (MGA)²⁹ in microstrip technology, for transmission and reception, mounted on an arm at the lower end of the satellite, deployed shortly after separation from the rocket (see figure showing the WIND satellite). There are also low-gain hemispherical beam receiving and transmitting antennas (two at each end of the satellite), which are used for the launch period, early satellite orbit and "contingency" (unforeseen) operations. The satellite records scientific and HK data onboard using two recorders. The satellite periodically communicates data to the ground at a high rate during tracking passes: about two hours of contact per day. One recorder is used at a time. During contacts with the ground tracking system, the recorded data are returned, while the second recorder stores the data for the next ground contact: this mode of operation is called "store and dump". Alternatively, the satellite can be made to provide data in real time for limited periods when the ground tracking system permits³⁰.
- **Propulsion subsystem:** this subsystem allows the impression of speed increases during the mission. The WIND satellite uses a propellant based on hydrazine (N₂H₄). Six tanks can store up to 395 kg of fuel. The satellite has eight thrusters for its speed increment maneuvers. These thrusters are arranged in the satellite in such a way that these thrusts do not cause the axis of rotation to deviate from its nominal orientation. The satellite's remotely controlled maneuvers use the internal propulsion system, which provides a velocity increment capability v greater than 500 m/s at the start of the mission.
- **Command and Data Handling System (C&DH).** This sub-system allows, thanks to different equipment (attitude and command processors, telemetry modules, recorders, etc.), the execution of all the satellite's remote controls (in real or delayed time). It processes and records the satellite telemetry data for on-board recording or for sending data in real time.

Note: eclipse periods

The WIND/Waves software library (§ 2-4) provides "items" (WIND_SA_MAX_AMPS_R4 and WIND_SA_MIN_AMPS_R4) corresponding to the current collected by the solar arrays of the satellite (these data are CDF data). The interest of this information lies in the fact that it allows to detect with precision the eclipse periods. In such cases, the current is at a minimum.

The orbit data would lead to a less accurate estimate of these periods.

Eclipse periods are of particular interest for scientific analysis (e.g. lunar wake studies). Moreover, the photoelectrons emitted by the satellite interfere with data reception, which is not the case during eclipse periods.

The curve of the current collected by the solar panels during the eclipse of 27/12/94 is shown below (to be drawn).

²⁷ The star chosen is Canopus in the constellation of the Carina. The reason for this choice is that this star is easy to spot. It is identified by its brightness.

²⁸ Communications are in S-band, compatible with the DSN network. TBW. VHF telemetry (136-138 MHz) in S-band (approx. 2 GHz). Also VHF or S remote control.

²⁹ Medium Gain Antenna (MGA) are intermediate between Low Gain Antenna (LGA) and High Gain Antenna (HGA), like the one found on the Ulysses probe. LGA antennas have a very wide angular coverage (practically omnidirectional), at the expense of a low gain. HGA antennas, with a parabolic reflector, have a high gain, but a very small angular coverage (fraction of a degree). The larger the collecting area of

³⁰ This possibility is important when the satellite is used for the detection and prevention of disturbances caused by solar activity (see § 1-2-4).

1.2.4. Detection and prevention of solar disturbances

WIND measurements can be used for the advanced detection and prevention of solar-induced terrestrial disturbances. The array of satellites flying over the different key regions of the IP and geospace environment, in particular those belonging to the ISTP program, as well as the ground observation stations, allow the detection and monitoring of such events (solar flares, CME, magnetic clouds, geomagnetic storms, ...) on a very large scale. During the operational life of the WIND satellite, the following significant solar events can be reported:

- Event of October 18-20, 1995: on October 18, 1995 at 19:00 UT, the WIND probe, then located at 175 R_e above the Earth, detected an interplanetary disturbance of very high intensity: "giant magnetic cloud"³¹. The cloud was heading towards the earth at a speed of 370 km/h, when it was detected by WIND. The cloud was preceded by a shock wave between 10:40 and 19:00 UT. It hit the Earth's magnetic shield 30 minutes later. It was also detected by the GEOTAIL³² satellite. On contact with the Earth's magnetic shield, this disturbance produced a magnetic storm and auroral phenomena for two days.
- January 6-11, 1997 event: On January 6, 1997, an intense earthward-flowing Coronal Mass Ejection (CME) forming a halo around the sun as a result of its expansion, was captured by the visible light coronagraph LASCO on board the SOHO satellite. The front of the giant magnetic cloud, traveling at 450 km/s, was detected by the WIND probe on January 10 at 04:45 UT, identified by the SWE and MFI experiments, the IP shock arriving shortly before 01:00 UT. On January 10, 1997, this cloud collided with the Earth's magnetic shield generating a magnetic storm and intense aurora borealis, observed in northern Europe and Canada. This event was observed by about twenty satellites, including POLAR and GEOTAIL, and about thirty ground-based instruments³³.
- Event of April 7-11, 1997: On April 7, 1997, a large flare followed by a CME was detected by EIT and LASCO at 14:00 UT (flare at 14:00, CME at 15:00 UT). The WIND/Waves experiment detected a type III flare at 13:59 UT, followed by a type II flare. On April 11, CANOPUS and POLAR also detected this event. Auroras were observed over the Earth as far as the latitude of Boston.

These events occur more frequently during the active period of the 11-year solar cycle³⁴. Larger geomagnetic storms can be expected as this activity increases to a maximum around 2000-2001. The Space Environment Laboratory (SEL) Prediction Center of NOAA, located in Boulder (Colorado), the official agency of the American government, has the objective of predicting such events. NOAA alerts various organizations around the world that may be affected by these disturbances, in particular commercial satellite operators and power companies ("space weather alert"). Its long-term objective

³¹ A magnetic cloud is characterized in particular by a strong magnetic field that varies little, in contrast to the magnetic field carried by the solar wind which is highly fluctuating and about five times less intense. Magnetic clouds are only occasionally directed towards the earth.

³² See for example: COSPAR, Information bulletin, No. 135, April 1996.

³³ The American communication satellite Telstar 401 (AT&T), saw its operation definitively deteriorate the next day, which could be a consequence of this CME [e.g. Le Monde of 01/02/97]. NASA announced later that other satellites, especially military ones, had also been damaged. The magnetic cloud put a strong pressure on the lines of force of the earth's magnetic field. The pulse compressed the magnetosphere on the solar side by about 1/3 of its length, or 23 000 km. This event, which received significant scientific and media coverage, was the subject of a workshop in April 1997 at the GSFC.

³⁴ We are currently at the end of solar cycle 22, so at a minimum of solar activity. These events are not the most important ones that we have had to observe. We can recall in particular the event of March 1989 during the last period of solar activity, which put out of order the electrical systems around Quebec, plunging its 6 million inhabitants into darkness, and deviating several satellites from their orbit.

would be to forecast the arrival of a disturbance from the sun sufficiently in advance (one to two weeks). Many forecasting centers³⁵ around the world, created since the 1960s, are involved in this study. This has been called "space weather". DESPA is also involved in this type of program³⁶.

In the case of the October 1995 event, the CME was detected by the WIND probe while it was transmitting its data to the ground ("tracking pass"), which occurs only two hours a day. This coincidence allowed the LRS to immediately launch an alert. In order to make this possibility almost permanent, the forecasting specialists have placed an additional transmitter on board the ACE satellite, launched in August 97, and positioned at the L₁ Lagrange point, for a data transmission from three ACE instruments³⁷ ("NOAA REAL Time Solar mission") to the ground receiving stations managed by NOAA, when this satellite is not transmitting its data to the ground, about 21 hours out of 24, with a telemetry rate of 464 bps. In this way, it will be possible to be informed of the arrival of a disturbance at ground level about half an hour to an hour in advance, depending on the speed of the disturbance [NEW96].

It appears that, in general, the links between classical solar physics, CMEs, interplanetary disturbances and magnetic storms are not obvious³⁸. In the coming decade, NASA's SEC program will attempt to answer these questions. From a scientific point of view, the analysis of such data allows us to study how interplanetary disturbances propagate and affect the Earth's environment. The event of January 10, 1997, for example, generated the first type II burst observed by the WIND probe (see dynamic spectrum). Contrary to what one could expect, the EPACT instrument on the WIND probe did not observe an increase in proton and electron energy fluxes.

Dynamic spectrum of 8/1/97

³⁵ There are ten Regional Warning Centers (RWCs) around the world, belonging to the International Space Environment Service (ISES) network, which collect data from their geographical area and disseminate them to the ISES network. The Meudon observatory hosts one of these centers. The Boulder center is particular in that it is a World Warning Agency center.

³⁶ The INSU has set up a national program, one of whose themes is solar "meteorology" (SHET: Sun, Heliosphere and Earth Environment).

³⁷ These three instruments are: EPAM (Electron, Proton, and Alpha Monitor), SWEPAM (Solar Wind Ionic Composition spectrometer), and MAG (Magnetometer).

³⁸ This is the case for the event of January 6, for example. The sun did not show any really striking features on that day. A DSF (Disappearing Filament) and weak coronal activity south of the center of the solar disk were observed around noon on January 6. See the Appendix.

1.2.5. Experiments on board the WIND probe

We describe here the experiments on board the WIND probe, which are described in detail elsewhere [SSR95]. We refer to figure 1 for a visualization on the satellite of the sensors associated with these various experiments.

1-2-5-1 Description of the experiments

Ion analysis

- The Energetic Particles: Acceleration, Composition and Transport (EPACT) experiment studies acceleration and transport processes during solar flares, in the interplanetary medium and the Earth's magnetosphere. It determines the abundance, elemental and minor isotopic composition of high energy ions in the solar wind. Because of their high charge, these ions can be used as tracers for the transfer and flux of particles from the solar wind to the magnetosphere. This experiment includes the three telescopes: LEMT (Low Energy Matrix Telescope system), ELITE (ELECTron Isotope TElescope system), and STEP (SupraThermal Energetic Particle telescope). The energy range covered is from 0.2 to 500 MeV.
- The SMS (Solar Wind and Suprathermal Ion Composition and Mass measurements) experiment aims to determine the abundance, velocity, composition and differential energy spectra of solar wind ions, as well as the composition, charge and three-dimensional distributions of supra-thermal ions. The study of these ions allows a diagnostics of events at the solar surface, as a complement to the EPACT and 3DP experiments. The three main instruments are: SWICS (Solar Wind Ion Composition Spectrometer), STICS (Supra-Thermal Ion Composition Spectrometer), and MASS (High Mass Resolution Spectrometer). The energy range covered is 0.5 to 500 MeV.

Ion and electron analysis

- The 3DP (3D Plasma and energetic particles investigation) experiment is designed to obtain the complete three-dimensional distribution of solar wind electrons and suprathermal ions, from a few eV to several hundred keV, between the solar wind range and the low-energy cosmic ray range, covering a wide range of directions. It studies particle acceleration, upstream of the Earth shock and in the pre-shock region, transient particles emitted by the sun following solar flares, transport phenomena, and basic plasma processes (wave-particle interaction, type III bursts, Langmuir waves, shock waves, non-linear processes, solar wind heat flux). The experiment consists of three detector systems: the Solid State Telescope (SST), the Electron ElectroStatic Analyzer (EESA) and the Proton ElectroStatic Analyzer (PESA). The EESA and PESA sensors are mounted on two 40 cm long radial booms ("boomlets") to avoid the potential effects of the satellite on the detection of low energy particles and to allow a large angular field. In addition, the Fast Particle Correlator (FPC) instrument combines density information from the Waves experiment with data from the electron analyzer to study wave-particle interactions.
- The Solar Wind Experiment (SWE) studies the properties of ions and electrons in the solar wind and ion-electron pre-shocks. The experiment provides three-dimensional velocity distributions that reveal the properties of plasma flows and their pivotal role in the transfer of mass, momentum and energy from the sun to the earth. The instrument has two Faraday slices, designed by the MIT Center for Space Science, that allow the deduction of solar wind velocity, density and temperature of protons and alpha particles from the solar wind at energy-to-charge ratios *up to 8 kV*. The instrument also contains a detector array built by the GSFC to characterize the electrons in the solar wind.

Wave analysis

- The Waves experiment, which is the subject of this document, is designed to study radio waves and plasma phenomena in the solar wind upwind of the Earth and in the magnetosphere. It measures low frequency electric waves (continuous to 10 kHz): FFT instrument, thermal noise from 4 to 256 kHz: TNR instrument, radio waves from 20 kHz to 14 MHz: RAD1/2 instruments, and can sample waveforms very quickly: TDS instrument. The Waves experiment is connected to the three magnetic antennas ("search coils") and to the three electrical antennas of the satellite.
- The MFI (Magnetic Field Investigation) experiment studies the large-scale structure and fluctuations of the interplanetary magnetic field that influence energy transport and particle acceleration in the solar wind and dynamic processes in the magnetosphere. The direction of the magnetic field is critical to understanding the interactions between the solar wind and the Earth's magnetosphere. The experiment uses a fluxgate magnetometer. The data from the MFI experiment are used in the interpretation of the other WIND experiments.

Gamma-ray burst analysis

- The TGRS experiment (Transient Gamma Ray Spectrometer) is designed to detect gamma-ray bursts³⁹. These events occur in the 15 to keV range at 8.2 MeV and at great distances from the Earth.
- The KONUS experiment is designed for studies similar to TGRS on gamma-ray bursts, and complementary in energy coverage. The experiment is designed for the study of gamma-ray bursts, and can also analyze solar flares in the hard X-ray range. The instrument is a gamma-ray spectrometer, composed of two identical detectors.

These two gamma-ray spectrometers provide the first high-resolution spectroscopic coverage of transient cosmic gamma rays, including those from solar flares, X-ray novae, and other sources.

1-2-5-2 Summary table of experiments and contractors

On board the WIND satellite are eight scientific experiments. Of these, six are American, one, Waves, is Franco-American, and one, Konus, is Russian. This is the first Russian instrument to be carried on an American satellite.

³⁹ Gamma-ray spectrometers study cosmic gamma-ray bursts. Gamma-ray bursts are very brief transient bursts of gamma rays. The ignorance of their origin, object of many theories (neutron stars, extra-galactic origin, ...), makes them one of the mysteries of contemporary astrophysics [see for example Le Monde of 25/04/97].

Type of experiment	Name	Title	Scientific objective	P.I.	Project manager
Waves	MFI	Magnetic Field Investigation	Interplanetary magnetic field fluctuations	R. Lepping	NASA/GSFC
	WAVES	Radio and Plasma Waves	Radio and plasma wave measurement	J-L Bougeret Mr. Kaiser	Observatoire de Paris - University of Minnesota
Particles (ions, electrons)	SWE	Solar Wind Experiment	Ion and electron distribution functions	K. Olivigie	NASA/GSFC
	3D PLASMA	3 Dimensional Plasma and Energetic Particles Experiment	Particle acceleration at the sun, particle transport in the IP environment	R. Lin	University of California, Berkeley
	EPACT	Energetic Particle: Acceleration, Composition, and Transport	Ion and electron distribution functions	T. Von Rosenvinge	NASA/GSFC
	SMS (SWICS, MASS, STICS)	Solar Wind and Suprathermal Ion Composition and Mass measurements	Ion charge, temperature and velocity	G. Gloekler	University of Maryland
Gamma rays	TGRS	Transient Gamma Ray Spectrometer	Gamma-ray bursts	B. Teegarden	NASA/GSFC
	KONUS	Gamma Ray Burst Investigation	Gamma-ray bursts	E. Mazets T. Kline	Ioffe Physical Technical Institute, St. Petersburg, Russia. NASA/GSFC

1.3. The Waves Experiment

1.3.1. Project milestones

The WIND experiments were selected, after competitive review, by NASA in 1980, in response to the "Announcement of Opportunity"⁴⁰ for the former OPEN program. Funding for the GGS project was approved by the US Congress for a re-launch in 1988. The main milestones of the WIND/Waves project from the Congress's decision to launch are as follows (see DESPA space research proposals, Waves experiment, by J-L Bougeret):

January 1988	Relaunch approved for the ISTP/GGS program.
February 1988	Updating of calls for tender.
Oct/Nov 1988	Establishment of the new ISTP project team.
November 1988	General Electric/ Astro Division selected as prime contractor for WIND probes and POLAR
December 1988	Official confirmation of teams and PIs. J.L. Bougeret P.I. of the Waves experiment.
July 1989	SRR (Spacecraft Requirement Review).
September 1989	PDR (Preliminary Design Review) for the experiment Waves.
November 1989	PDR for WIND and POLAR probes.
December 1989	PDR for Waves antenna mechanisms.
May 1989	Critical Design Review (CDR) for Waves antenna mechanisms.
June 1990	CDR for the Waves experiment.
December 1990	PDR (Preliminary Design Review) for on board the Waves experiment.
September 1992	PER for Waves.
June 1992	Flight Model (FM) qualification.
June 1992	PSR for the Waves experiment.
September 1992	Delivery of the MV to General Electric.
September 1992	PSR for antennas.
December 1992	Integration of the MV on the satellite.
November 1 st , 1994	Launch of the WIND probe.

In the context of an on-board space experiment, the following stages are defined chronologically and more or less formally: design of the tabletop model (feasibility study of an instrument), the identification model (or "Engineering Model"), during the development phase of the instrument, whose physical and electrical configuration is identical - hence its name - to the final configuration, and the Flight Model (FM), manufactured in a clean room.

The "commissioning" phase, after the probe has been placed in orbit, took place in November 1994. During this period, it is verified that the satellite is functioning properly and that it is capable of carrying out its assigned mission. Once this phase is completed, the satellite is declared operational and routine operations begin []].

1.3.2. First maneuvers

The main highlights of the Waves experiment in the first few days after the launch are as follows:

01 November 1994	Launch at Cape Canaveral (10:31 a.m.).
------------------	---

⁴⁰ A space mission at NASA consists of several phases. During the pre-phase A, or conceptual study, NASA forms a Science Working Group (SWG). A scientific document ("Announcement of Opportunity") is sent to the various centers (universities, scientific organizations, NASA centers, etc.). This is followed by phase A, or preliminary analysis, phase B or definition phase (conversion of the preliminary analysis into a technical solution), phases C/D (design and development), and finally the operational phase.

	Deployment of the MGA communication antenna
09 November 1994	Deployment of “search coils” ⁴¹
10 November 1994	Simultaneous motorized deployment of the two LDBs supporting the DC and AC magnetometers, reaching their full length in about 45 minutes ⁴² . The Waves experiment started without any particular problems.
11 November 1994	Formal start of the instrumental activation phase with a switch to "Science" telemetry format. Deployment of E_x wire antennas (about 48 minutes) and E _y (approximately 8 minutes 20 seconds) ⁴³
16 November 1994	First perigee (1.43 R _e). Phasing maneuver at 10:31 GMT.
18 November 1994	Deployment of the E_z.

1.3.3. scientific objectives and applications

The purpose of the Waves experiment is to provide measurements characterizing plasma and radio waves in the solar wind, over a frequency range from nearly DC (continuous) to about 13.825 MHz. Specifically, the science fields envisaged are []:

- Location of the source of the solar wind and its physical characteristics as it approaches the Earth. Flux interactions between the fast and slow solar winds. Heat flux carried by solar wind electrons and anisotropic instabilities.
- Formation of interplanetary shocks. Acceleration of sub-relativistic particles in coronal shocks. Impulse phenomena related to shock waves. Upstream waves and fluctuations, generated by energetic electrons and ions accelerated at the Earth shock.
- Local measurement of plasma characteristics (absolute calibration of density, temperature and velocity). Plasma instabilities and wave-particle interactions.
- Radio mapping of the heliosphere. Structure of the interplanetary magnetic field. Correlation of the radio observations of Waves with those of the ULYSSES/URAP experiment. Contribution of the radio technique to the whole ISTP program, and in particular to SOHO (LASCO, E.I.T) and CLUSTER experiments.
- Low frequency antenna impedance, behavior of electric antennas in sunlight.

Current scientific applications of the Waves experiment include the following studies:

- Solar bursts

Study of type III bursts: low frequency limit, radiation diagram. Correlation of

⁴¹ The magnetic sensors are located at the end of an [articulated](#) arm at the end of the LDB. This arm is deployed before the LDB itself. The deployment of the LDBs is accompanied by an increase in speed (from 7 to 20.5 revolutions per minute).

⁴² The extension of the masts, once the satellite has separated from the launcher, is a particularly critical phase in a space mission. Among other things, it requires changes in the satellite's attitude and rotation speed. Various disappointments have been experienced during various space missions due to the malfunction of the deployment system, even though the satellite is otherwise perfectly functional. For other satellites, the deployment of the solar panels, the telemetry antenna (as for the Galileo probe), or the parabolic antenna reflector are also critical phases. [As for the mast supporting the magnetometers, it is stored in a very compact way. Once deployed, it cannot be retracted \[OEH\].](#)

⁴³ It can be seen that the deployment time is a direct function of the antenna length.

WIND/ULYSSES/ARTEMIS measurements (J-L Bougeret, G. Dulk, S. Hoang, Y. Leblanc, M. Poquérousse).

Study of type III with Langmuir waves. Direction and polarization of radio sources. WIND/ULYSSES and WIND/GEOTAIL triangulation (S. Hoang et al.; M. Reiner et al.).

Type II bursts - correlation with MEC (J-L Bougeret).

- Planetary bursts

Analysis of Jovian bursts (A. Lecacheux; P. Zarka et al.).

- Solar wind

Measurement of plasma characteristics by QTN analysis (M. Maksimovic, C. Perche).

Nonlinear phenomena and coherent wave packets in the solar wind.

- Plasma waves

TDS instrument and nonlinear theory in the pre-shock. Langmuir waves (S. Bale, P. Kellog et al.).

- Various

- Lunar wake study (P. Kellog et al.).

Waves observations of terrestrial radio transmissions. (J-L Bougeret, M. Kaiser).

The goal of the Waves⁴⁴ experiment is to analyze these measurements, in coordination with other on-board measurements of plasma, energetic particles and fields.

We refer to:

- "Waves-2", the part of the Waves experiment designed and built by the University of Minnesota School of Physics and Astronomy laboratory, which includes the FFT, TDS and DPU instruments.
- "Waves-1", the part of the Waves experiment designed and built by DESPA at Paris-Meudon Observatory, which includes the RAD1, RAD2 and TNR instruments.

The Waves-1 experiment uses two types of measurements: in situ measurements (thermal noise measurement, TNR instrument), and remote sensing measurements⁴⁵ (radio analysis of the interplanetary medium, RAD1 and RAD2 instruments).

⁴⁴ The Waves experiment is also called "Radio and Plasma Waves Investigation".

⁴⁵ When the waves produced do not propagate (electrostatic waves), as in the case of thermal noise, they can be detected locally: this is called in situ analysis. When they do propagate (electromagnetic waves, also called radio waves for the wavelength range we are dealing with), they can be detected at a distance: this is called remote sensing.

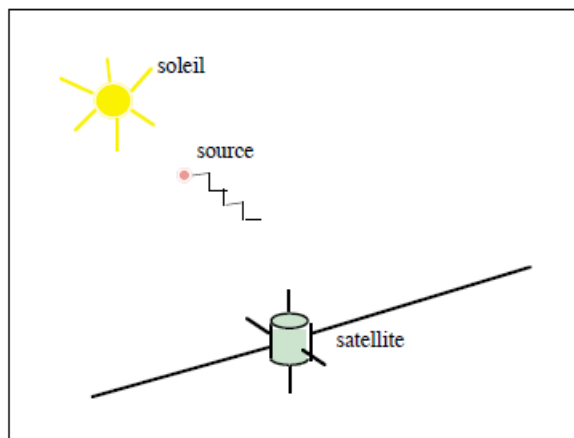


Fig. 1-3: remote sensing of radio waves

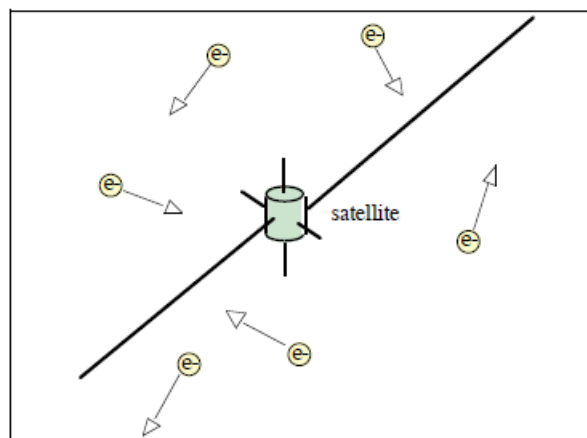


Fig 1-4: in situ thermal noise measurement

With the RAD2 receiver, the Waves experiment covers the frequency range from 1.075 to 13.825 MHz (decametric-hectometric band), which has never been successfully explored before. As noted by G. Dulk, observations in the range from 20 MHz, the low-frequency limit of terrestrial observations, to about 2 MHz, where satellite observations begin, were relatively few before WIND⁴⁶. It should be noted that this spectral range is difficult to study because it includes significant terrestrial radio emissions from human activity (terrestrial radio transmitters). In particular, this means that it is not possible to use an Earth-orbiting satellite to cover this frequency range.

The ARTEMIS radiospectrograph⁴⁷, also called RAD3 in the Waves experiment, with a frequency range of about 14 MHz to 570 MHz in the ecliptic plane, completes the frequency range of the on-board instruments. A complete radio coverage of the heliosphere is thus made possible, in the framework of what is usually called "ground-space synergy".

In France, the decametric array of the Nançay radioastronomy station (Observatoire de Paris, Sologne, Cher) has an array of 144 antennas that allows daily solar radio observations in the 20-80 MHz range [BOI80] and can therefore also be used as a source of ground-based data⁴⁸.

⁴⁶ This frequency band corresponds approximately to the regions of acceleration of the solar wind. It is in these regions that the solar wind originates. The range 1 to 10-15 MHz corresponds to heliocentric distances of 3 to 20 solar radii. The ISEE-3 mission has shown that it is also in this region that some large interplanetary shocks are formed, and that sub-relativistic particles appear [CEL88]. The SBH experiment of this mission allowed a satisfactory resolution up to 512 kHz, but insufficient beyond. (frequencies 1000 kHz, and 1980 kHz). The type III interplanetary storms, whose study allowed the measurement of the solar wind speed [BOU], can also be followed in the high corona, in the high corona, during solar maximum.

⁴⁷ The ARTEMIS ground equipment (Routine Apparatus for Magnetic Processing and Magnetic Recording of Spectral Information Spectral Information), managed today by the University of Athens ("Greek Center of Space Communications", Termopiles Station) [MAR93].

⁴⁸ Under the responsibility of P. Zarka, possibility of production of daily files if necessary.

1.3.4. Main participants and distribution

The Waves experiment is managed by a consortium whose main participants are the Observatoire de Paris (Meudon), the University of Minnesota (Minneapolis), the Goddard Space Flight Center (GSFC/NASA, near Washington, D.C.) and the University of Iowa (Iowa City). These four partners are responsible for instrument development. This collaboration, initiated during the ULYSSES/URAP mission, is continuing in the framework of the WIND/Waves mission. The division of tasks between the different participants is as follows:

Name of the laboratory (Organization)	Responsibility
Space Research Department – DESPA (Paris-Meudon-Nancay Observatory)	RAD1, RAD2, TNR, power converter, Electric preamplifiers: Waves-1.
School of Physics and Astronomy (University of Minnesota)	FFT, TDS, DPU instruments: Waves-2 experiment.
Department of Physics and Astronomy (University of Iowa)	Magnetic antennas and associated preamplifiers.
Laboratory for Extraterrestrial Physics – LEP (GSFC/NASA)	Electrical antennas (subcontracted to Fairchild Space, Maryland), mass data processing.

The radio stimulus part of the GSE (Ground Support Equipment) is done at DESPA. The satellite simulator is designed at DESPA and the University of Minnesota. The data acquisition software for all test phases⁴⁹ is being developed by the University of Minnesota.

DESPA is both the project manager, under the technical responsibility of Robert Manning, experiment manager for NASA, and the scientific co-leader of the Waves experiment: Jean-Louis Bougeret (DESPA) and Mike Kaiser (GSFC) are alternately P.I. (Principal Investigator) and deputy P.I. of the Waves experiment.

Several levels of verification of the health and safety of the instruments can be distinguished: the evolution and the long-term trend, the inspection of the daily summary plots, the Housekeeping data, the monitoring by the POCC, which for example can inform about the shutdown of an instrument.

The *GSFC* Waves team routinely monitors the operation of the experiment, checks the internal calibrations (K. Goetz), develops the software that produces the key parameters for the CDHF, and provides the NSSDC with these parameters in a timely manner (C. Meetre).

1.4. General description of the instrument

The electromagnetic sensors on board the WIND probe include electric wire antennas and magnetic search coils and fluxgate antennas. The Waves receivers process the signals from the electrical antennas, in the case of Waves-1, and from the electrical and magnetic antennas, in the case of Waves-2.

⁴⁹ Software library ("WIND library"), remote control system "icp", among others.

1.4.1. Electric antennas

1.4.1.1. General characteristics

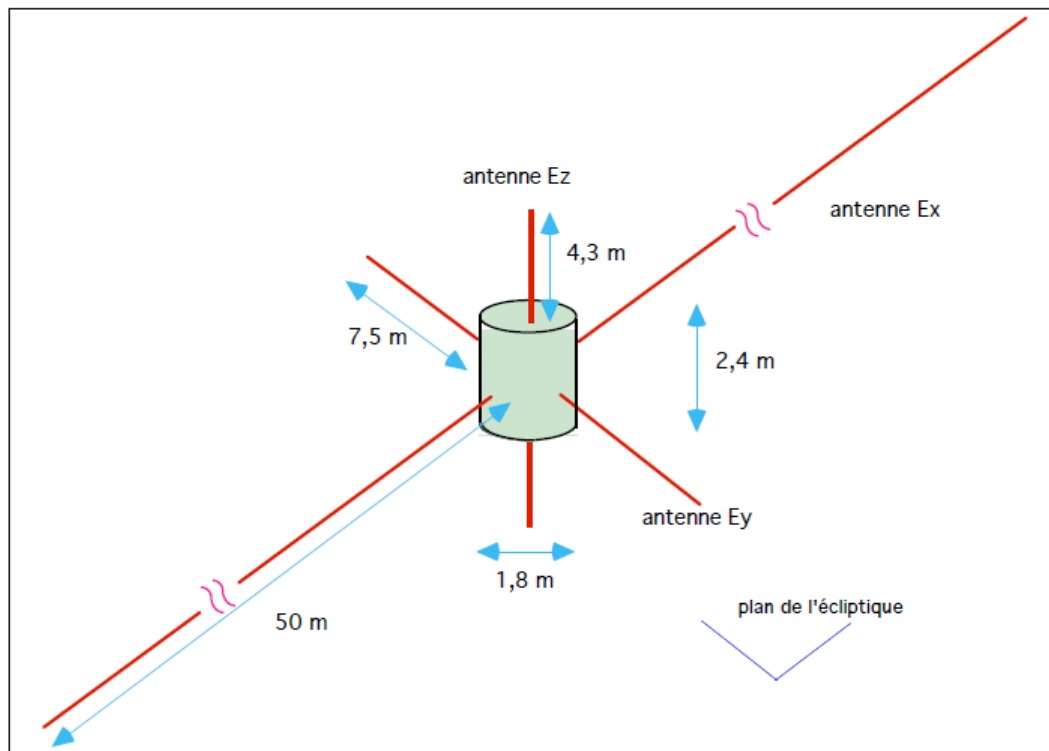


Fig. Electrical antennas on the WIND probe

There are three electrical antenna (dipole) systems⁵⁰, each consisting of two arms:

- two electrical antennas designated E_x and E_y , deployed after launch, orthogonal to each other, coplanar, located in the plane of rotation of the satellite (so-called radial or equatorial antennas). Each boom (monopole) constituting these antennas is fixed to the body of the satellite. The antennas are of different lengths to allow different spectral coverage. The E_x antenna is long: 2×50 m, and used for low frequency measurements (20 to 1040 kHz band, RAD1 receiver). The E_y antenna is short: 2×7.5 m, and used for high frequency measurements (1.075 to 13.825 MHz band, RAD2 receiver). These antennas are very thin (0.4 mm diameter). Their mechanical stability is ensured by centrifugal force.
- A rigid tubular electrical antenna designated E_z , oriented along the axis of rotation (Z axis) of the

⁵⁰ Two types of antennas are generally used on rotationally stabilized probes: "wires" antennas as shown here, which consist of a dipole (combination of two monopoles), and "sphere" antennas where two spheres are placed at the ends of a wire. Sphere antennas are more suitable for low frequencies (<10 kHz) and are particularly suitable for electrostatics. Indeed, their radiation pattern shows multiple lobes for too long lengths. For the Waves experiment, they also have the following disadvantage: the noise due to the collection or emission of particles by the antenna is of the same order as the QTN and the spheres must be supported by masts and wires which modify the field distribution and the impedance [MEY]. As an example, wire antennas can be found on ISEE3, ULYSSES and WIND and sphere antennas on GEOS and CLUSTER. The advantage of wire antennas is their light weight, ease of deployment or rewinding of the wire wound on a spool. Space constraints on the probes sometimes require the use of a monopole antenna rather than a dipole antenna (the ULYSSES probe has a monopole antenna along the Z axis). This arrangement has the disadvantage that the absolute potential of the probe is not known with sufficient accuracy: it can be known to within a few 0.1 V, whereas continuous measurements require an accuracy of more than a millivolt. This mainly affects very low frequency (quasi-continuous) measurements: low field continuous measurements are not possible. Low-field AC measurements are marred by the inaccuracy of the electrical reference [BOU93-a].

satellite (so-called axial antenna). One antenna boom (monopole) extends from each end of the satellite. The length of the E_z antenna, initially planned to be 2×5.28 m, has been reduced to 2×4.30 m since the launch, due to stability problems (satellite nutation). On 6 November 1996, the length of this antenna was increased by 2×35 cm, from 2×4.30 cm to 2×4.65 cm⁵¹. This antenna has a maximum total deployed length of 2×6.5 m. Its diameter is 2.84 cm.

N.B. the lengths indicated do not take into account the dimensions of the satellite itself.

Electric antennas are light and flexible elements whose weight and moment of inertia are negligible compared to those of the satellite, so that they do not influence its attitude, regardless of their deflection. On the other hand, they must be sufficiently rigid to allow for straightness of the antenna at rest and sufficient damping to avoid long periods of oscillation after a satellite maneuver. The antennas are stowed at launch and deployed on command when the satellite reaches its orbit.

Each monopole is connected to a preamplifier, so there are six preamplifiers in all. The preamplifiers are located in the immediate vicinity of the base of the deployment mechanism of each dipole⁵².

1.4.1.2. Configuration - Direction of rotation

The X, Y and Z axes of the satellite are defined as follows: the positive +Z axis is parallel to the axis of rotation, and oriented towards the south. The X and Y axes are perpendicular to the rotation axis and perpendicular to each other, forming a direct trihedron (right-handed coordinate system). This coordinate system is fixed with respect to the satellite body and therefore rotates at the same speed as it.

⁵¹ In general, it is desirable to have the longest E_z antenna possible in order to increase its sensitivity. This sensitivity varies in fact as approximately l^2 to l^4 where l is the length of the antenna. However, the dipole must remain short compared to the wavelength. The choice of length of the antenna is limited by the following theoretical constraint: the further away from the antenna resonance, the more the radiation pattern shows this is because the side lobes are detrimental to the directivity of the antenna, even though the antennas here operate in reception and not in transmission. In addition, restrictions on the length of the E_z antenna are imposed by considerations of dynamic stability of structures along the axis of rotation of a satellite, particularly during satellite thrusts. These restrictions lead to a lower sensitivity of the Z channel. The probe having consumed part of its fuel became lighter; the increase in size of the E_z antenna of 6/11/96 was thus made possible. Finally, the use of rigid antennas is necessary for a three-axis stabilized probe, and especially, as in this case, for an axial antenna on a spin-stabilized probe.

⁵² The signal is amplified in the PA, located as close as possible to the antenna terminals. This proximity is very important to minimize the effects of base capacitance. On one hand, this is to avoid the degradation of the signal-to-noise ratio caused by losses in the transmission line that carries the signal between the antenna and the PA (these losses are proportional to the length of this line); on the other hand, this line may itself act as an antenna and pick up interfering noise [BOU].

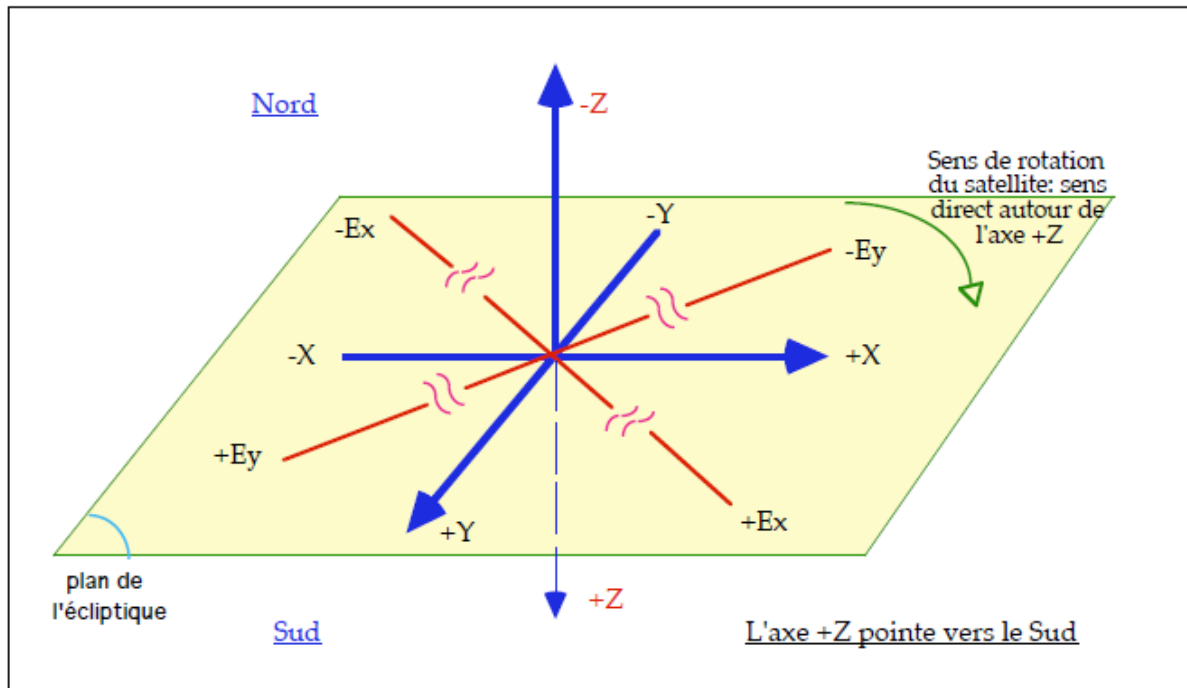


Fig. Arrangement of the electrical antennas in relation to the satellite axes (top view)

- The antennas in the rotation plane are not aligned with the satellite's X,Y coordinate system, but are offset by 45°. Their position, relative to the satellite axes, is shown on this diagram, see [ICD92] p 85.
- The direction of rotation of the satellite is direct⁵³ about the +Z axis **facing south**.

1.4.1.3. Modeling

The impedance of an electrical doublet can be developed in series as a function of as follows:

$$Z_a = \frac{1}{jC_a\omega} + R + jL_a\omega + A\omega^2 + \dots$$

C_a : static impedance of the antenna.

R : loss resistance (0 for an antenna assumed to be perfectly conductive).

L_a : self-inductance of the antenna whose reactance is very small compared to C_a .

The equivalent diagram of the antenna is as follows:

⁵³ The positive (or direct or trigonometric) direction is counterclockwise. The vector product: X Y is equal to Z when the X turns to the Y axis in the direct direction, and to Z in the opposite direction.

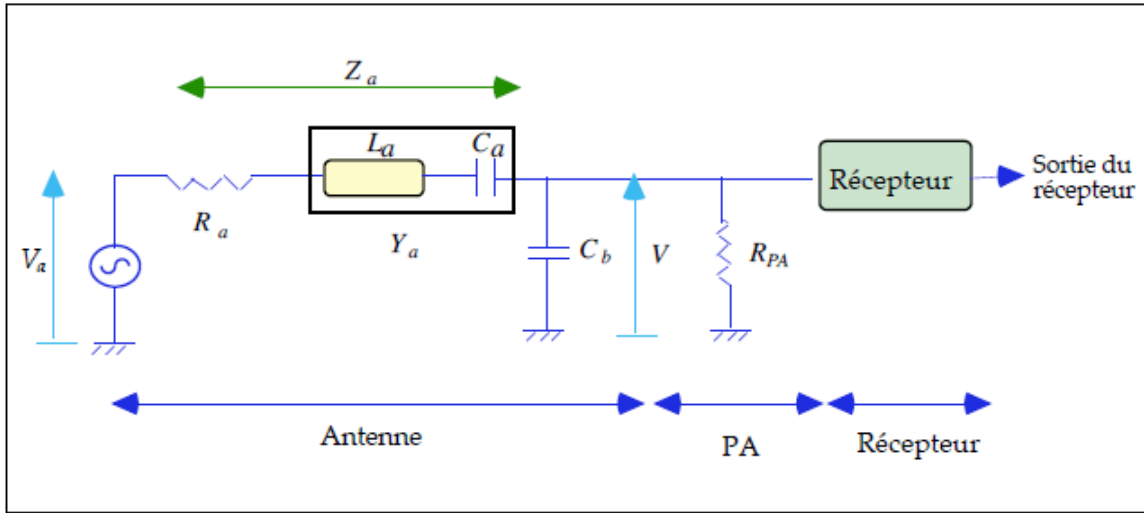


Fig. Equivalent electrical diagram of a WIND electrical antenna

The antenna impedance⁵⁴ Z_a comprises a radiation resistance R_a , and a reactance⁵⁵ Y_a , consisting of a capacitive part C_a and an inductive part L_a . The antenna is capacitive at low frequencies and inductive at high frequencies. The basic capacitance of the antenna is C_b . The input resistance of the preamplifier, R_{PA} , very high, is usually "ignored".

Let E be the electric field intensity (expressed in *Volts / m*) through the antenna and V the voltage measured across the antenna. Let V_a be the open circuit voltage across the antenna. We have, by definition of the effective length of the antenna:

$$V_a = E \cdot l_{eff} .$$

The standard analysis of this electrical circuit then allows us to deduce the following equation [DES95]:

$$E = \frac{\left(\omega^2 C_b^2 R_a^2 + (\omega C_b Y_a - 1)^2 \right)^{1/2} V}{l_{eff}}$$

The determination of the electric field strength therefore requires the knowledge of the effective electric length l_{eff} of the antenna. The values are given in the table in § 1-4-1-5.

1.4.1.4. Antenna capacitance

In the case of a distance from the local plasma frequency ($f \gg f_p$), the antenna capacitance C_a can be calculated theoretically (theory of a cylindrical dipole in an isotropic medium) and the antenna resistance. The antenna capacitance can be considered as equal to its value in vacuum, depending on the length and radius of the antenna, according to the following formula:

⁵⁴ It is recalled that the impedance of a capacitor of capacitance C_a is written $Z = 1 / jC_a\omega$. The impedance of an inductor of inductance L is written: $Z = jL\omega$.

⁵⁵ In the expression for a complex impedance $Z = X + jY$, Y is called the reactance.

$$C_a = \frac{\pi \epsilon_0 L}{\ln(L/a) - 1}$$

With: L : length of an antenna boom.
 a : radius of the antenna.
 $\epsilon_0 = 8.85419 \cdot 10^{-12}$ dielectric permeability of vacuum.

A more precise expression of this expression can be found in [JAS61].

Thus we have:

Antenna	Antenna capacitance value
E_x	$121.7 \cdot 10^{-12} \text{ F} \cong 122 \text{ pF}$
E_y	$21.9 \cdot 10^{-12} \text{ F} \cong 22 \text{ pF}$
E_z	$25.30 \cdot 10^{-12} \text{ F} \cong 25.3 \text{ pF}$

When the condition: $f \gg f_p$ is not respected, the antenna impedance depends on the physical characteristics of the ambient plasma around the antenna. These can be obtained, in the framework of the Waves experiment, by spectroscopic analysis of the thermal noise collected by the antenna. This technique allows to determine the electron density, the electron and proton temperature, and the overall solar wind speed (see chapter 5). Such a possibility supposes that the data from the TNR receiver have been processed beforehand.

1.4.1.5. Base impedance

The base capacitances C_b represent stray capacitance that can severely limit the sensitivity of the experiment. They are measured on the ground on the antennas themselves⁵⁶ as accurately as possible [MAN]. The base capacitance measurements of the 6 monopoles were made using a *vector voltmeter*. Considering the different physical components: coaxial cable, connectors, ..., between the antenna and the receiver, one can consider the following equivalent circuit for the antenna base impedance (model tested from 1 to 60 MHz):

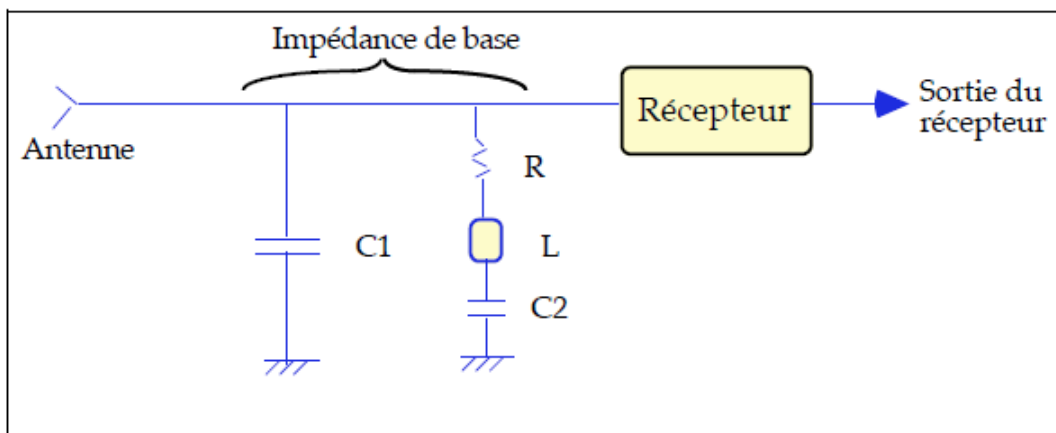


Fig. Equivalent circuit for the base impedance of the antennas

⁵⁶ For the ULYSSES/URAP experiment, direct measurement on the antennas had not been implemented. The base capacitance values obtained for the WIND probe are better than for the ULYSSES probe, because the preamplifiers are of better quality. The measurements obtained for the WIND/Waves antennas were the subject of an e-mail from R. Manning, (2/11/93) to which reference may be made.

The results are as follows:

Monopole	C ₁ (pF)	R (Ohm)	L (μH)	C ₂ (pF)	C ₁ +C ₂ (pF)
+ E _x	7.7	8.3	0.59	32.8	40.5 +/- 1
- E _x	7.3	8.6	0.59	32.5	39.8 +/- 1
+ E _y	7.0	9.2	0.61	32.7	39.7 +/- 1
- E _y	8.2	9.2	0.64	32.5	40.7 +/- 1
+ E _z	52.3	2.4	0.31	37.6	89.9 +/- 1
- E _z	49.3	5.7	0.30	37.8	87.7 +/- 1

The above values for base capacitances are those measured in dipole configuration, so the base capacitances of monopoles are twice as high⁵⁷.

At low frequencies, only the base capacitance C₁+C₂ is retained. Thus we have:

Base capacitance (C₁+C₂) of the equatorial wire antennas: 40 +/- 1 pF (for 1 monopole) AC
 Base capacitance (C₁+C₂) of the axial antenna: 88 +/- 3 pF

It should be noted that an accurate estimate of the base capacitance is more important for the RAD2 receiver, as the E_y antenna has a low antenna capacitance. The above values may need to be corrected for the magnetometer boom (TBC). These error bars include the uncertainty due to antenna deployment.

1.4.1.6. Summary Table

	Type	Material	Dipole length	Diameter	Long effective	Antenna capacitance (dipole)	Base capacitance (dipole)
E _x antenna	Motorized wire antennas	Bare Copper-Beryllium (BeCu)	2 x 50 meters	0.4 mm (or 0.38 mm: TBC)	2 x 41 m (TBC)	121,689 pF	20 pF (or 33 pF TBC)
E _y antenna	Motorized wire antennas	Bare Copper-Beryllium (BeCu)	2 x 7,5 meters	0.4 mm (or 0.38 mm: TBC)	2 x 5 m (TBC)	21.886 pF	20 pF (or 33 pF TBC)
E _z antenna	Retractable rigid motorized hose	Copper-Beryllium (BeCu) silver plated ribbons	2 x 4,3 meters	28 mm (or 2.84 cm TBC)	?	25.30 pF	44 pF (TBC)

Remarks:

- Studies are underway to determine the exact value of the base capacitance: it can be 20 or 33 pF (see calibration chapter).
- RMS length values are not yet very accurate due to interference from magnetometer booms.
- Further information on these measures can be found in Chapter 5.

⁵⁷ These are the inverses of the capacitances that add up; the two monopoles being identical, the capacitance of the dipole is half the capacitance of the monopole.

1.4.2. Magnetic field measurements

1.4.2.1. Magnetic antennas

The measurement of the low-frequency *alternating* magnetic field (fluctuations of the magnetic field with respect to an average) is performed by means of a tri-axial alternating induction magnetometer⁵⁸ (search coils) designed and built by the University of Iowa and used by the FFT and TDS (Waves-2) instruments. The magnetometer consists of three coils mounted at the end of the 12 m long Lanyard Deployable Boom (LDB), oriented in the -X direction of the satellite. The three search coils are contained in the lanyard canister at launch and released in their normal operational position after deployment of the LDB (the booms are stowed during launch and deployed on command), once the satellite has been placed in orbit. The interplanetary magnetic field to be measured is very weak (a few nanoTeslas) and the magnetic fields produced by the satellite's electric currents are strong enough to interfere with these measurements: the magnetometer must therefore be placed at the end of a long boom, away from these interferences.

These three single-axis sensors are arranged orthogonally in directions parallel to the electric antennas so that the magnetic field is measured in the same coordinate system as the electric field. Each is 40.6 cm long. Pre-amplifiers are incorporated into the sensor mechanism and are located in the immediate vicinity of the sensors, so there are three pre-amplifiers in all. Each sensor delivers a signal proportional to the strength of the magnetic field component aligned with it. Thus, by associating three sensors, along three perpendicular axes, it is possible to measure the instantaneous magnetic field. We have the following diagram (from [CNE94] p. 713):

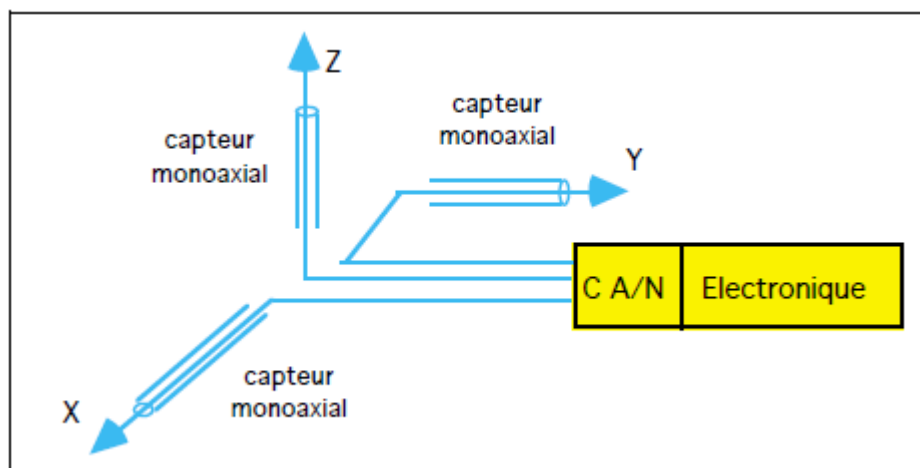


Fig. Principle of magnetic antennas

The magnetometer measures the magnetic field over a frequency range from 0 to 2.7 kHz. The associated frequency response peaks at about 1.6 kHz. The magnetometer, with its preamplifiers, is similar to the one designed for the POLAR mission.

- Also on the satellite is a tri-axial DC field magnetometer (fluxgate type, MFI experiment, [LEP95] p. 218) allowing measurement of the static magnetic field in the range $[+/-0.001 \text{ to } +/-65\,536 \text{ nT}]$. Like the induction magnetometer, it is placed⁵⁹ on a boom (the LDB) 12 m long, but in the opposite

⁵⁸ Winding of a very large number of turns around a core of high magnetic permeability μ (ferromagnetic material). The operating principle of magnetometers is based on Faraday's law. The voltage induced across a winding of N turns is written $V = N \cdot S \cdot dB/dt$, where S is the surface area of the turns, B the magnetic field (assumed here to be uniform). Any variation in the ambient magnetic field leads to a variation in the magnetic flux and therefore to the appearance of an induced voltage. An electronic integrator circuit is then used to obtain B .

⁵⁹ In practice, there is an external unit at the end of the LDB and an internal unit halfway between the external magnetometer and the satellite body. This configuration allows for the estimation and real-time elimination of the dipole components of the magnetic

position (+X) to the boom supporting the induction magnetometer, and is deployed in flight. The length of the boom is such that at this distance, the continuous residual magnetic field due to the satellite is only +/- 0.1 nanoTesla.

The diagram of the satellite in § 1 confirms the -X and +X directions of the arms supporting the magnetometers.

1.4.2.2. Azimuth and magnetic elevation

The direction of the static magnetic field B measured by the DC magnetometer can be characterized by two angular quantities: the magnetic elevation and the magnetic azimuth. The magnetic azimuth is obtained as follows: when the +X axis, on which the continuous magnetometer is located, is aligned with the projection of B on the (X,Y) plane, the perpendicular component B_y is cancelled by decreasing. The detection of this zero crossing gives rise to a pulse called MagAz: the magnetic azimuth is thus obtained by comparison with the "Sun reference pulse". The magnetic elevation will be obtained as follows: the corresponding pulse named MagEl is emitted N clock pulses after the MagAz pulse.

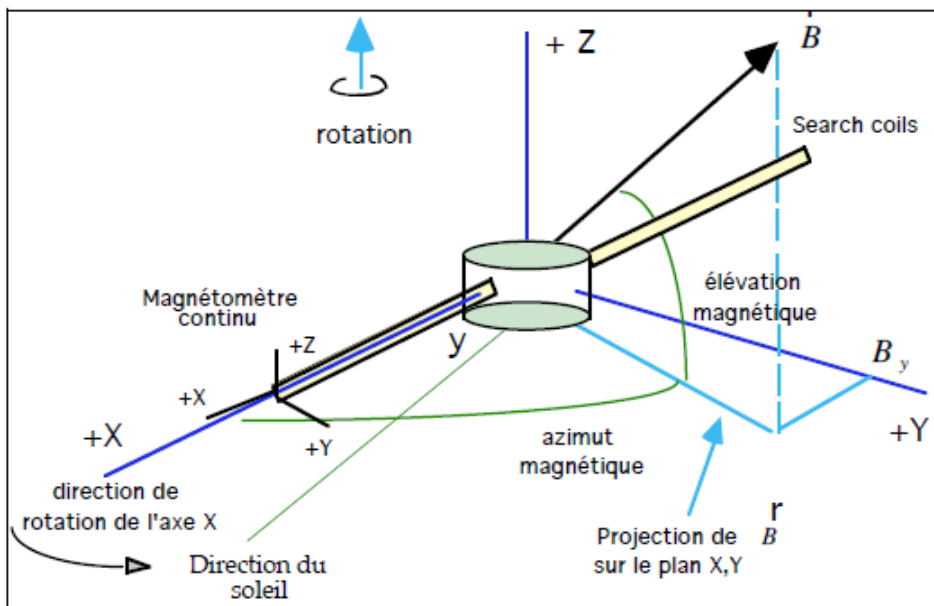
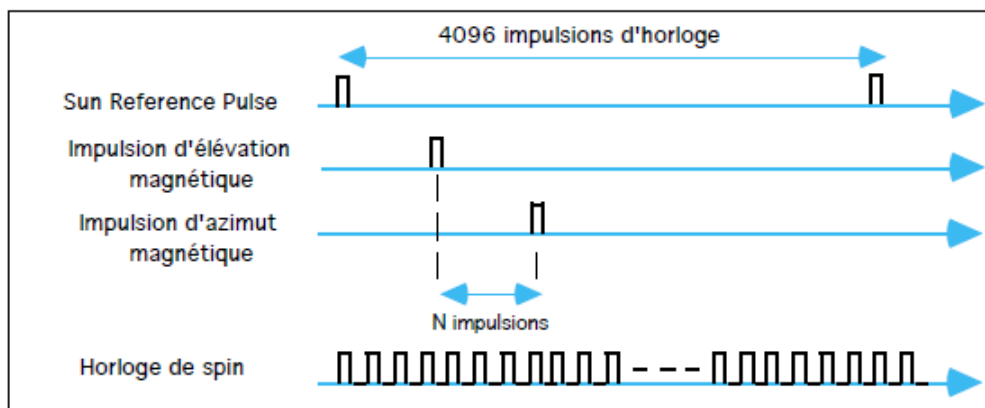


Fig. Azimuth and elevation (from [1])

The time diagram is as follows:



1.4.3. Solar Impulse

The sun sensor mounted on the probe is aligned⁶⁰ with the +X axis of the probe. The "Sun Reference Pulse" (SRP, or "sun pulse" or "solar top" or "solar pulse"), a pulse emitted by this optical sensor, occurs when the +X is directed towards the sun. This pulse is translated into the appropriate information in the telemetry. The clock rate of the satellite clock is 4096 Hz. This means that in one rotation between two sun tops, the clock delivers 4096 pulses⁶¹. This results in an accuracy of $1/4096 = 0.244 \text{ Hz}$.

Note: during an eclipse, it is obviously no longer possible to obtain this information, but the satellite continues to send this information at the same rate as before the eclipse.

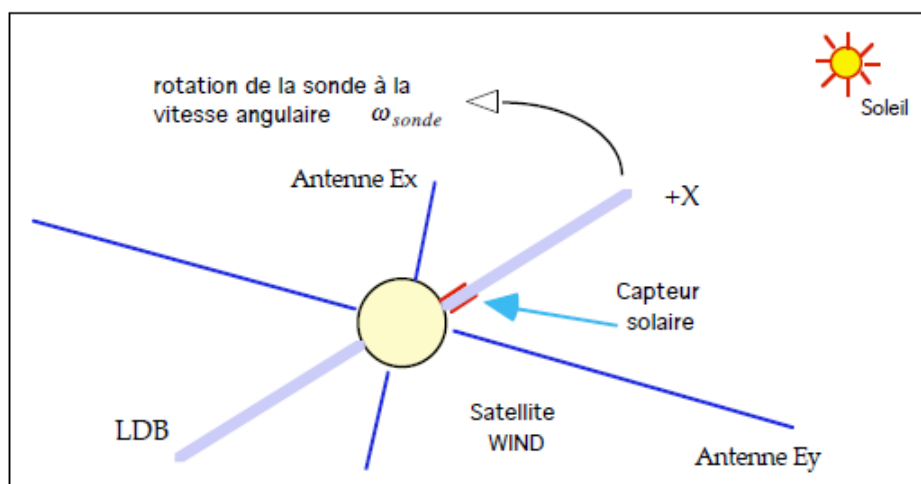


Fig. Sun reference pulse and satellite layout

At the time t , the angle $\Delta\Phi(t)$ at which the probe has rotated with respect to the direction of the sun is obtained by multiplying the angular velocity of rotation of the ω_{sonde} with the time difference $\Delta t = t - t_{soleil}$ between the time t considered and the time t_{soleil} of the solar pulse:

$$\Delta\phi(t) = \omega_{sonde} \cdot (t - t_{soleil})$$

At the level of the WIND/Waves software library (see above), the following "items" can be found:

- SUN_ANGLE: This "item" gives for each event the number of clock pulses at the start of the event. This value goes from 0 to 4095. It is 0 when the +X of the probe (boom of the continuous magnetometer) is directed towards the sun (TBC).
- SUN_ANGLE_R4: This "item" gives for each event the angle to the sun at the start of the event. The angle is given in degrees. We have the relation:

$$\text{SUN_ANGLE_R4} = \frac{\text{SUN_ANGLE}}{4096} \cdot 360^\circ$$
- WIND_SPIN_RATE_R4: This "item" gives average angular velocity in radians/s. This information is taken from the KP. For a nominal rotation of 3.096 s, the rotation speed is: 2.02945 radians/s.

⁶⁰ This is not systematic. On the Cluster probe for example, the solar sensor is located at 18.6° from the magnetometer boom.

⁶¹ With the necessary corrections, using oscillators, which take into account the previous rotation so that there are 4096 pulses at the next rotation.

1.4.4 The Waves Experiment

1.4.4.1. General scheme

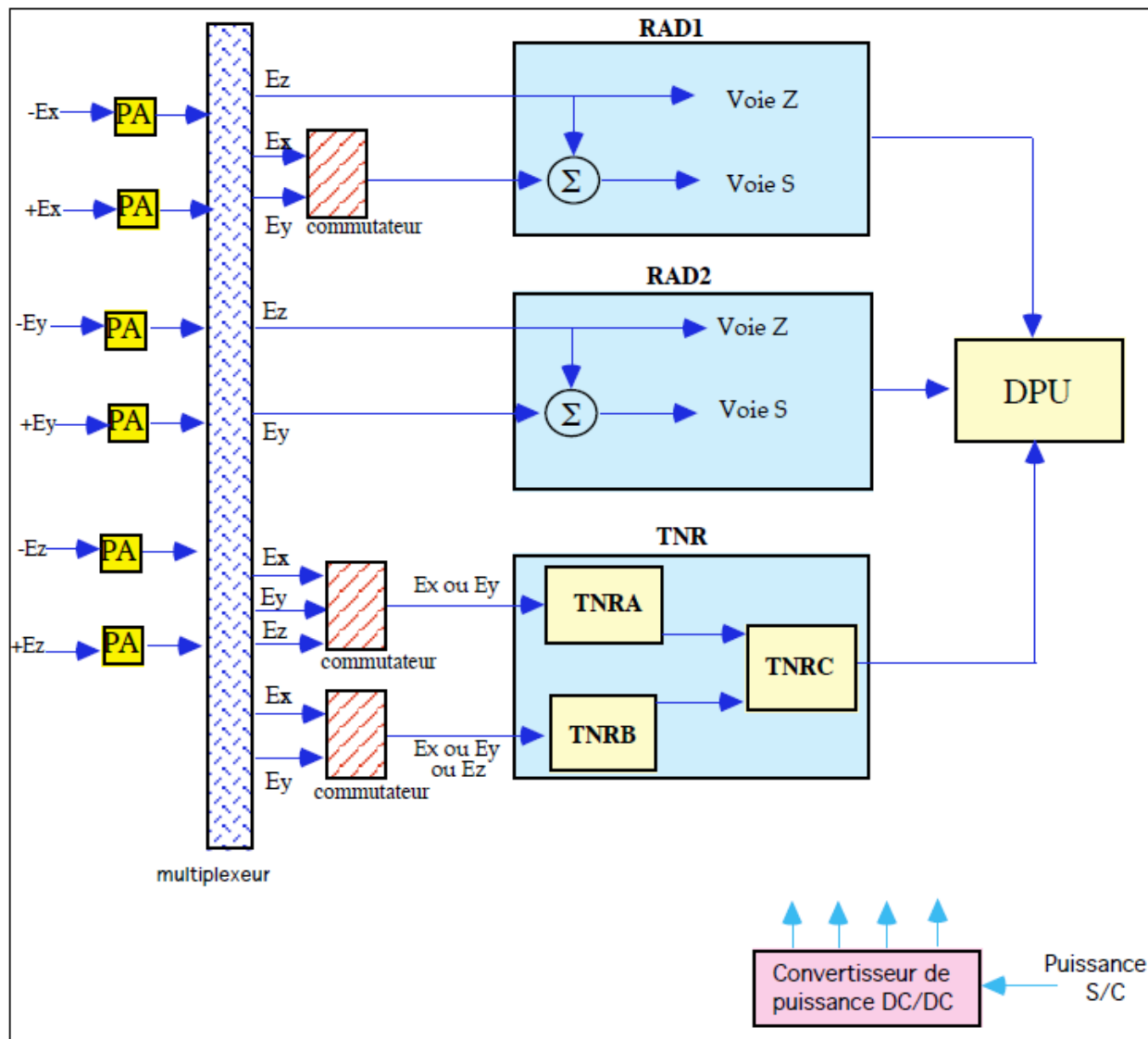
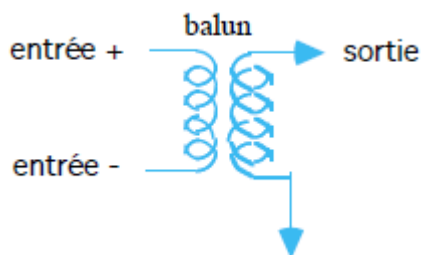


Fig. Schematic diagram of the Waves experiment

“Baluns” (“balanced-unbalanced”), not shown above, are used to switch between the + and - inputs of the antennas/PAs at the output.



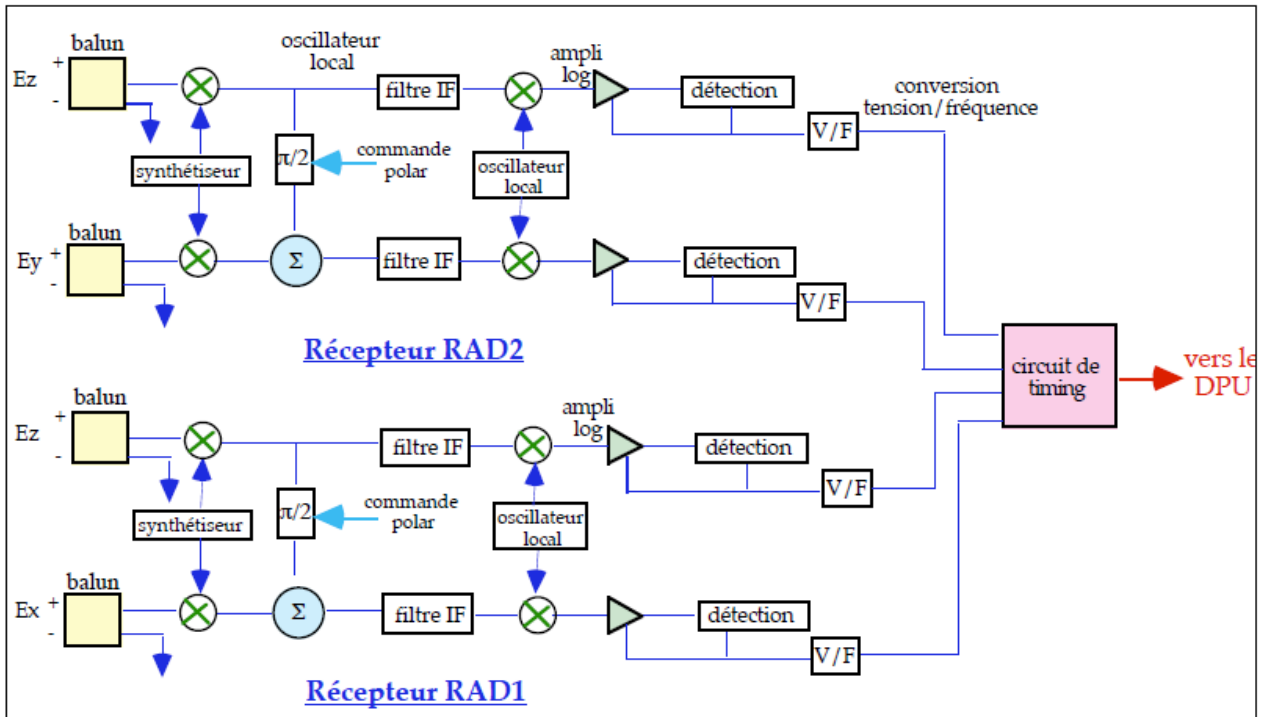


Fig. Block diagram of RAD2 and RAD1 instruments

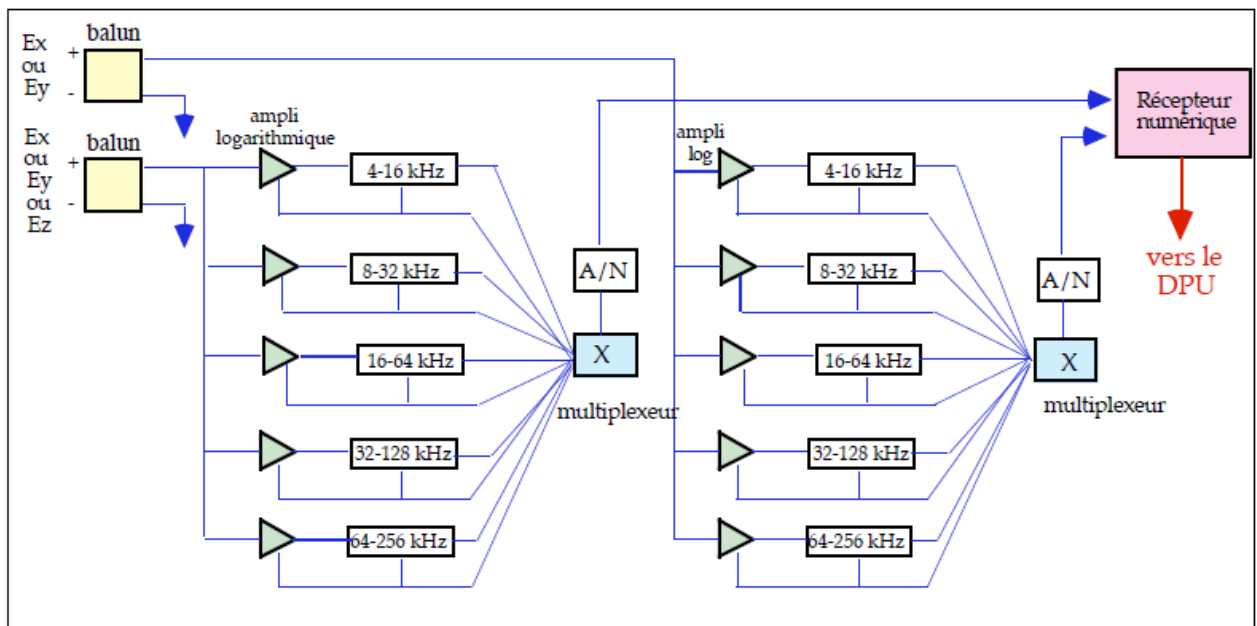


Fig. Block diagram of the TNR instrument

1.4.4.2. Weights of the individual components

The masses of the various components of the Waves experiment are as follows:

Sensors

Sensor	mass	number of units
Wire antenna (50 m)	3,45 Kg	2
Wire antenna (7.5 m)	3,35 Kg	2
Axial antenna (6.5 m)	6,5 Kg	2
Magnetometer	0,3 Kg	3

Subtotal for sensors: 27,5 Kg

Electronics

Sensor	mass	number of units
PA	0,2 Kg	6
Waves-1	5,8 Kg	1
Waves-2	8,7 Kg	1

Subtotal for electronics: 15.7Kg

Cumulative total (electronics + sensors): 43,2 Kg

This mass is relatively high mainly due to the antenna mechanisms. The weight and size problems of the instruments and boxes are taken into account.

The main electronics of the Waves instrument are included in two batteries (Waves-1 and Waves-2) that the manufacturer can place anywhere in the main body of the satellite.

1.4.4.3. Input floors

The electrical voltages induced at the antenna terminals by the weakest sources we wish to detect are of the order of a few hundred nanovolts; they must therefore be strongly amplified, avoiding the introduction of noise as much as possible, before being detected and recorded.

It has been shown that the noise of an entire receiving chain depends on the first receiving stages, and essentially on the first electronic stage, i.e. the preamplifier. Indeed, the noise temperature of a receiver comprising n stages, with respective noise temperatures T_1, T_2, \dots, T_n , and of respective gain G_1, G_2, \dots, G_n , is given by the *Friis* formula:

$$T_{\text{récepteur}} = T_1 + \frac{T_2}{G_1} + \frac{T_3}{G_1 G_2} \dots + \frac{T_n}{G_1 G_2 \dots G_n}$$

The preamplifier is the first element in the receiving chain, and the result is that the preamplifier is the first element in the receiving chain:

$$T_{\text{récepteur}} \approx T_1 = T_{PA}$$

The amplifier stage is an important element of the acquisition chain in that it conditions the sensitivity of the whole acquisition chain⁶². The aim is to obtain a preamplifier with both good linearity and good sensitivity [KNO79].

In the Waves experiment, each preamplifier has three outputs: one with a gain close to unity for the RAD2 instrument, a second with a gain shared by the TNR, RAD1, RAD2, FFT, and TDS instruments, and a final one with unity gain for the TDS and D/C.

Each preamplifier has two outputs: a gain output for the higher frequency part of the instrument provided by DESPA and a gain output close to the unit for Waves-2. These preamplifiers are similar to those built for the ULYSSES mission.

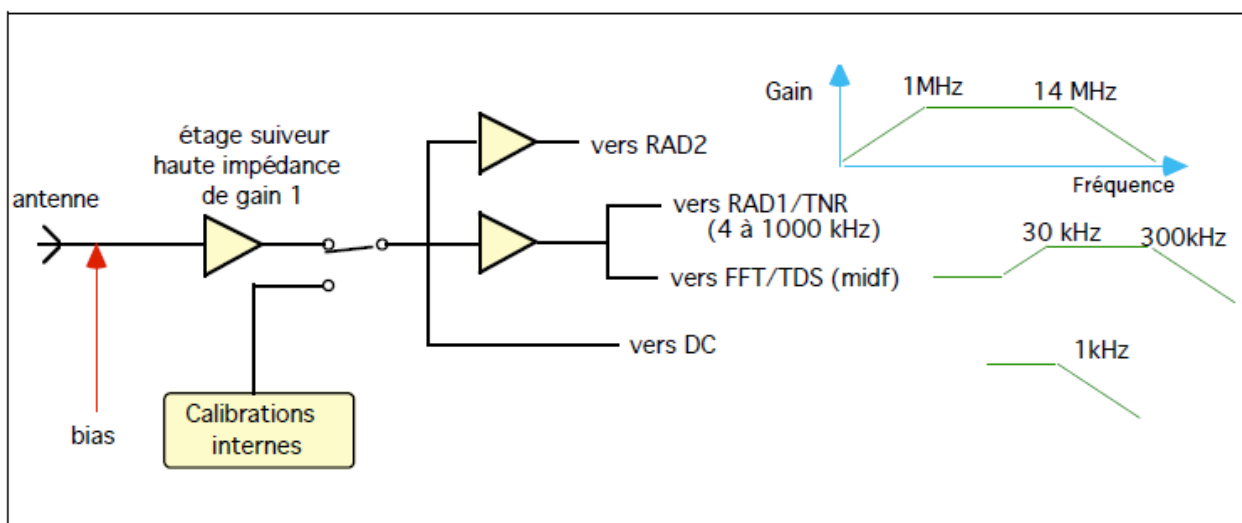


Fig. Waves input stage: preamplifiers for electrical antennas

The purpose of the "follower" stage (high impedance, unity gain) is to reduce the input noise. When a zero value signal is applied at the input, a certain voltage value is obtained at the output, called the "bias", which is re-injected at the input.

1.4.4.4. Power converter

DESPA is responsible for the fabrication of a DC/DC power converter for the whole Waves experiment. It is similar to that of the ULYSSES/URAP experiment. The role of this converter is to power the different parts of the experiment. It is physically located in the "stack" containing the Waves-1 experiment. The EMI emissions of this converter are very low. Some redundancies in the design improve the safety of the operation. Separate output stages (choppers, transformers, filters) are used for the major components of the experiment:

- PA,
- TNR, RAD1, RAD2,
- FFT, TDS, and search coils,
- DPU.

⁶² The more sensitive a receiver is, the weaker the signal it can detect. The lower the noise figure, the more sensitive the receiver.

1.4.4.5. Electromagnetic compatibility

Electromagnetic compatibility (EMC) is the ability of different electrical and electronic systems in the same assembly to operate simultaneously while avoiding the effects of mutual electromagnetic interference (EMI). The systems must not only be free of interference, but also effectively protected against interference from external circuits. Currents flowing in the satellite circuits cause interference that is detrimental to the reception of weak signals, and particular care must be taken in the shielding of cables and the design of on-board equipment, especially certain circuits such as the power converter or the telemetry encoder. In the context of equipment manufacture, this means that these issues have to be considered at a very early stage of the satellite design⁶³.

Within the framework of the WIND and POLAR missions, electromagnetic compatibility aspects have been the subject of a special program to reduce interference effects as much as possible (magnetic, electrostatic and electromagnetic cleanliness). This is to allow precise measurements of very low energy plasma and low intensity electric and magnetic fields. Various protective measures and ground definitions have been taken (a single common ground, power supplies delivering multiple frequencies of 50 kHz only, EMI tests in anechoic chamber, etc.). In addition, all the external surfaces of the satellite (solar panels, thermal coatings, etc.) are conductive so as to create an equipotential surface and constitute a Faraday cage protected from the radiation of electric fields [HAR95]. These precautions make it possible to guarantee a sufficient level of sensitivity, for example for the TNR instrument which collects a relatively weak signal.

1.4.4.6. Sources of background noise

Knowledge of the various sources of noise that can affect instrumental measurements in flight is important. Indeed, this knowledge makes it possible to adjust the sensitivity threshold of the instruments, to foresee the measurements that can effectively be carried out without being drowned out by the noise, and during the processing of the ground data, to subtract the background noise from the emissions that we are trying to study (useful signal). The noise observed in flight is essentially the result of three types of noise:

- On the one hand, the noise related to the external environment, namely:

- "Astrophysical" noise (or galactic or cosmic noise). It comes from various unresolved galactic radio sources. Galactic noise comes from interstellar gas in the galaxy. It is very high in low frequency, up to 1 GHz. Its frequency spectrum is continuous and smooth, peaking at about 3 MHz and decreasing rapidly towards the lower frequencies (see figure at the end of § 1-5-7).
- Noise due to photoelectrons generated by the satellite under the impact of solar radiation. It is a low frequency noise.

On the other hand, the noise of the receivers, which comes mainly from the preamplifiers, see above.

⁶³ "It is now established that Electromagnetic Compatibility (EMC) problems must be taken into account from the design phase. On a system, addressing EMC from the early stages of a project avoids the need to dismantle cables or equipment, which is more a matter of one-off repairs than optimizing protection. On the other hand, a design approach which would systematically consist in faradizing the walls and using protection devices at the equipment entrance would lead to an increase in weight (detrimental to aircraft and spacecraft) and would make the systems much more delicate to monitor during their operational life (accessibility and maintenance problems)" [J-P Parmentier et al, "Topologie électromagnétique", REE magazine, n°4, p. 63, April 96].

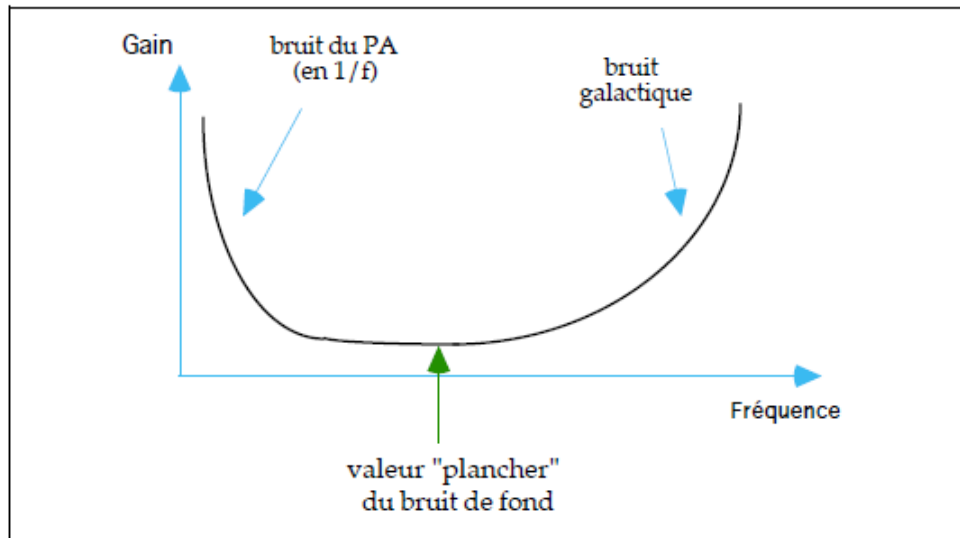


Fig. Background components.

The lower part of the curve indicates the minimum noise level. It is with respect to this floor value that a receiver must be adjusted: it is indeed useless to design a receiver whose sensitivity is better than this floor noise level. A possible variable attenuator at the input of the receiver will help to set the correct level.

See the concrete example of the RAD1 receiver on p. 281 and the figure at the end of § 1-5-7. 281, as well as the figure at the end of § 1-5-7. On these curves, check that the noise floor has a minimum around 200 kHz for a level between 10-20 and 10-21 Watts m⁻² Hz⁻¹.

1.4.4.7. Receivers

The signals collected by the various sensors are analyzed by an electronic assembly consisting of five quasi-independent receivers:

- part Waves-1:

a multi-channel broadband analyzer (4 kHz to 256 kHz), mainly intended for the study of thermal noise (in situ measurements), called **TNR** (Thermal Noise Receiver). This receiver, which contains a signal processing microprocessor, provides measurements of the thermal noise spectrum with high temporal and spectral resolution. *Its sensitivity is limited only by galactic noise.*

two frequency-swept radio receivers for radio remote sensing measurements of the heliosphere⁶⁴, named **RAD1** (RADio receiver band 1) covering the low frequency range 20 kHz to 1040 kHz, and **RAD2** (RADio receiver band 2) covering the high frequency range 1 075 to 13 825 MHz.

- part Waves-2:

a low frequency wave analyzer (DC to 20 kHz) by fast Fourier transform, called **FFT** (Fast Fourier Transform).

A time domain sampler, with a sampling rate of up to 120,000 samples per second, called **TDS** (Time Domain Sampler). This high temporal resolution is intended to recognize events of very short duration, according to certain criteria programmed in the DPU.

The DPU, FFT and TDS instruments are equipped with the SA3300⁽⁶⁵⁾ microprocessor which offers

⁶⁴ The heliosphere is the theoretical sphere under the influence of the Sun.

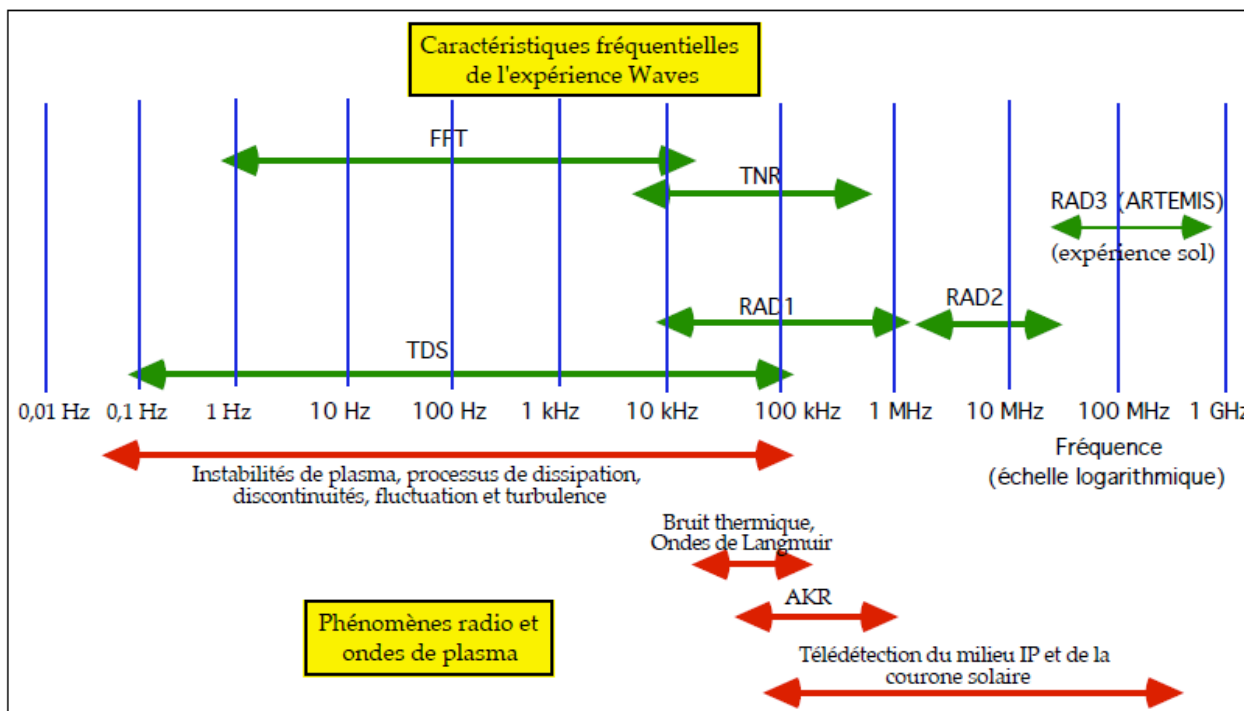
⁶⁵ Microprocessor manufactured by the company "Sandia National Labs" in CMOS technology, radiation resistant, equivalent to
Chapter 1 – Description

both power and ease of programming. In the case of the TNR receiver, the ADSP 2100 signal processing microprocessor from Analog Device was chosen.

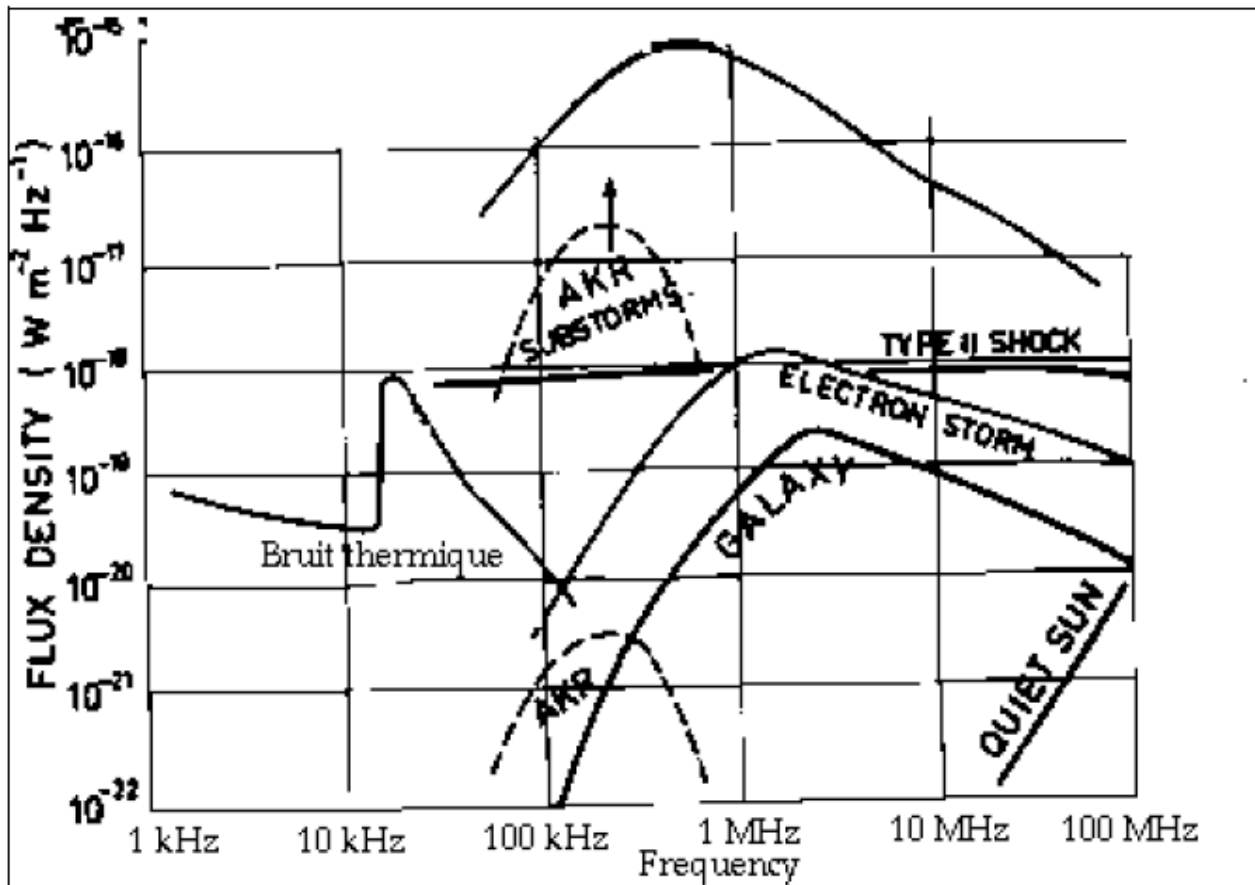
The summarized characteristics of the receivers are as follows:

	Antennas	Spectral range	Bandwidth	Number of channels	Dynamics	Sensitivity
RAD1	Ex + Ez, Ez	20 kHz - 1,040 MHz	3 kHz	256	approx. 70 dB	$7 \text{ nV} / \sqrt{\text{Hz}}$
RAD2	Ey + Ez, Ez	1.075 - 13.825 MHz	20 kHz	256	approx. 70 dB	$7 \text{ nV} / \sqrt{\text{Hz}}$
TNR	Ex, Ey or Ez	4 - 256 kHz	4.4% or 9% of center frequency	80 or 160 in 5 bands	approx. 100 dB	$7 \text{ nV} / \sqrt{\text{Hz}}$

Waves-1 Receiver Summary Features



Synoptic diagram of the frequency ranges of the different instruments of the Waves experiment and associated physical phenomena (from [BOU95])



According to J-L Bougeret:
Radio Waves in the heliosphere [Adv. Spa. Res., 13,6]

1.4.4.8. The DPU

The whole experiment is controlled by a central microprocessor, the **DPU** (Data Processing Unit). Its role is to:

- receive remote commands from the satellite and transmit telemetry data to the satellite.
- control and acquire data from the RAD1 and RAD2 receivers. These receivers do not have their own autonomy, it is the DPU that manages them: control of the operational mode, of the 256 frequencies synthesizer, of the SUM/SEP mode, of the antenna selection for RAD1, etc...
- control and acquire data from the TNR: antenna selection, operational mode, optimal frequency range.
- acquire data from TDS and FFT. Note that these instruments are equipped with their own microprocessor.
- transmit housekeeping information to the telemetry.

The DPU operating software is designed so that, in principle, any software module can be replaced by download.

The total memory used by the instrument is 126 Ko (ROM), 624 Ko (RAM).

1.4.4.9. Interfaces

There are four interfaces between the Waves experiment and the satellite:

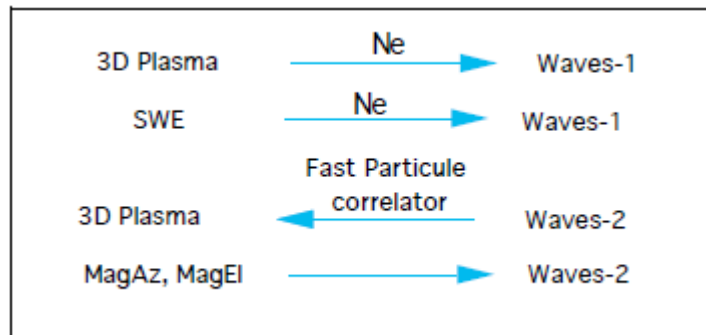
- 1) Local electron density signal N_e (first order moment of the electron distribution function) from the SWE experiment via a serial line: after a pre-defined time interval, the SWE experiment transmits a

coded number representing N_e . This number will be used by the DPU to help positioning the TNR instrument on the plasma line (AC).

2) Similar link from the 3D Plasma experiment to Waves-1 which shows the local electron density measured by the 3D Plasma experiment.

3) Waves-2 signals to the 3D Plasma experiment for the study of wave-particle correlations in solar plasma⁶⁶: two analog signals E_x , E_y from TDS are transmitted to the 3D Plasma experiment which performs a one-bit cross-correlation (i.e. correlation or non-correlation) between fields and particles, on fast timescales (a few microseconds) The Fast Particle Correlator (FPC) module of the 3D plasma experiment combines the electron data from the high sensitivity electronic analyzer and the data from the Waves experiment to study wave-particle interactions [LIN95].

4) Value of the static magnetic field measured by the continuous magnetometer (MFI experiment): MagAz (azimuth), MagEl (elevation). The Waves-2 experiment uses these data to define the FFT sectors.



1.4.4.10. Default receiver flight values

The various concepts discussed here will be developed throughout the paper.

RAD1/RAD2 receiver

	RAD1	RAD2
Antenna	E_x	E_y (no other choice possible)
Polar	Enable	Enable
Sum/sep	Sum	Sum
Linear scan mode	List	List
List of frequencies	0	0
Table of pointers	0	0
Start frequency (linear scan mode)	0	0
Frequency step (linear scan mode)	1	1
Number of steps (linear scan mode)	256	256

TNR receiver

Antennas	E_x connected to TNRA and E_y connected to TNRB (*)
Mode	mode 2 i.e. 32 channels/band, data from TNRA
Scanning	ACE
Number of spectra/event	12 (i.e.: ACE ACE ACE ACE)

(*) It can be seen from this table that in the default operating mode of the TNR (mode 2), where only data from the TNRA receiver are acquired, the data collected by the E_y antenna, connected by default to the TNRB receiver, are not taken into account.

⁶⁶ Beating phenomena between the frequency of the radio wave and the movement of the particles.

1.4.4.11. Immediate and non-immediate modes

Immediate and non-immediate modes are available for RAD1/2 and TNR instruments. Most of the commands have to take effect with a new packet, a new event, etc. (see chapter 2). Most of the time, one does not want a remote control to be taken into account during a measurement (non-immediate mode). On the other hand, you may want a remote control to be taken into account immediately (immediate mode).